JCTC Journal of Chemical Theory and Computation

Theoretical Investigation of Tautomeric Equilibria for Isonicotinic Acid, 4-Pyridone, and Acetylacetone in Vacuo and in Solution

Peter I. Nagy,*,† Giuliano Alagona,‡ and Caterina Ghio*,‡

Department of Medicinal and Biological Chemistry and Center for Drug Design and Development, The University of Toledo, Toledo, Ohio 43606-3390, and CNR-IPCF, Institute for Physico-Chemical Processes, Molecular Modeling Lab, Via Moruzzi 1, I-56124 Pisa, Italy

Received July 7, 2006

Abstract: Tautomeric equilibria have been theoretically calculated for isonicotinic acid (neutral and zwitterionic forms), the 4-pyridone/4-hydroxypyridine system, and the keto−enol transformation for acetylacetone in vacuo and in tetrahydrofuran, methanol, and water solvents. Solvent, basis set, and cavity model effects have been studied in the integral equation formalism for the polarizable continuum model (IEF-PCM)/B3LYP framework, as well as the effect of the procedure, CHELPG or RESP, applied in fitting atomic charges to the in-solution molecular electrostatic potential (ELPO). The in-solution optimized geometries obtained at the IEF-PCM/B3LYP/6-31G* and 6-311++G** levels differ moderately but deviate from their gas-phase counterparts. Atomic charges fitted to the in-solution ELPO show small variations in the considered solvents, as well as when the united-atom cavity model, or a model with explicit consideration of polar hydrogens and scaled Bondi radii, has been applied. In contrast, the fitting procedure considerably affects the derived charges producing more separated atomic charges when the CHELPG rather than the RESP procedure is utilized. The fitted charges increase up to 20% in absolute value when the basis set is enlarged from 6-31G* to 6-311++G** in the IEF-PCM/B3LYP calculations. The relative free energy, calculated as $\Delta G_{tot} = \Delta E_{int} + \Delta G(solv) + \Delta G_{thermal}$ + (symmetry correction), in an ab initio/density funtional theory (DFT) + free energy perturbation (FEP)/Monte Carlo (MC) approximation strongly depends on the accepted value for the relative internal energy, ΔE_{int}, of the tautomers. ΔE_{int} is to be calculated at the IEF-PCM/QCISD(T)/cc-pVTZ//IEF-PCM/B3LYP/6-31G* level for the isonicotinic acid tautomers for producing relative free energies in aqueous solution close to experimental values. In other solvents, for this system and for the other two tautomeric equilibria, calculation of ΔE_{int} at the IEF-PCM/B3LYP/6-31G* level produces ΔG_{tot} in agreement up to 1 kcal/mol with the experimental values. FEP/MC ΔG(solv) calculations provide robust results with RESP charges derived by a fit to the in-solution ELPO generated at the IEF-PCM/B3LYP/6-31G* level. Molecular dynamics simulations pointed out that isonicotinic acid forms a dimeric zwitterion in tetrahydrofuran, in contrast to what happens in aqueous solution, and this structural peculiarity was interpreted as the reason for the failure of the ab initio/DFT + FEP/MC method in this particular solution.

I. Introduction

Explicit solvent models of in-solution physicochemical processes use intermolecular potentials for calculating a large number of atomic interaction energies in most cases nowadays. Pure ab initio or density functional theory (DFT) calculations are not feasible (mainly at a high theoretical level and/or with large basis sets) for systems with medium-size solutes and several hundreds of solvent molecules. Such calculations are even less feasible for statistical averaging of millions of geometric arrangements for the members of the system. Although Car−Parrinello molecular dynamics simulations[1] have been performed for systems where all molecular interactions are considered at the DFT level,[2] the method has technical limitations at present for large systems.

A computationally more affordable method for modeling in-solution processes is based on the quantum mechanical/molecular mechanical (QM/MM) approach, where the system is divided into two regions characterized at different levels

* Corresponding author phone (419) 530-1945 (P.I.N.), +39-050-3152449 (C.G.); fax: (419) 530-1909 (P.I.N.), +39-050-3152442 (C.G.); e-mail: pnagy@utnet.utoledo.edu (P.I.N.), C.Ghio@ipcf.cnr.it (C.G.).

† The University of Toledo.

‡ Institute for Physico-Chemical Processes.

10.1021/ct6002252 CCC: $37.00
Published on Web 05/24/2007

of theory.[3] The region considered to be most responsible for the physicochemical process is described at a QM level. For the remainder of the system, and for considering the interactions between quantum and classical regions, MM approximations are employed. The MM methods make use of different approaches for calculating the intermolecular interaction energy. In force fields, one of the most important contributions is the electrostatic term: when atom−atom interactions are to be taken into account, atomic charges for the individual atoms or groups of atoms are needed in the different molecules. Accordingly, the simulation reliability may significantly depend on the selected set for the atomic (group) charge parameters.

QM/MM methods are used in cases where quantum effects are decisive in some region of the system. An obvious example is the study of chemical reactions when the breaking and forming of chemical bonds occurs. A "softer" problem is investigating conformational and/or tautomeric equilibria for a solute molecule. In these processes, only the relative free energies of some particular structures are to be calculated, and further simplifications are possible throughout the modeling.

In tautomeric equilibria, in particular, new chemical bonds are formed while old ones vanish. However, we are not interested here in the reaction mechanism involved in the tautomeric effect, but rather in the relative stability of the two forms in vacuo and in solution. Quantum chemical considerations are therefore requested, although only for some specific solute structures. On the other hand, the selected quantum-chemical level has to account also for the solvent effects in these cases.

The present authors have been investigating conformational/tautomeric changes in solution for a long time.[4] Net relative free energies were calculated as a sum of the relative internal and solvation free energies. It has become clear, however, that in order to reach accord with available experimental equilibrium constants obtained in different solvent systems, a sophisticated modeling approach is required. The mutual solute−solvent polarization modifies the electron distribution of the partners, and as a result, both the geometries and the relative internal energies change for the stable in-solution solute species as compared to their gas-phase counterparts.

When a polarizable continuum dielectric approximation is applied for a solution model, explicit structural changes can be reached for the solute. When this information is used, the net relative free energy for the conformational/tautomeric isomers of the solute can be obtained as a sum of the relative internal free energies calculated quantum chemically and solvation free energy changes obtained with some explicit solvent model. To get good values for the latter, determination of reliable solute atomic charges to be used in calculations of the solute−solvent interaction energies via pair potentials is needed. In the present investigation, the effects of different simulation parameters on the calculated free-energy changes for tautomeric transformations of isonicotinic acid, 4-OH-pyridine, and acetylacetone in tetrahydrofuran, methanol, and aqueous solution are studied. Net atomic charges derived for a solute molecule immersed in a polarizable continuum dielectric are compared. As variable modeling parameters, the cavity formation procedure, the quantum mechanical level as well as the basis set, and the methods employed for fitting net atomic charges to the in-solution molecular electrostatic potential were also considered. In Monte Carlo (MC) simulations with explicit solvent molecules, the effect of the applied charge sets and the approximations used for calculating the long-range electrostatic interactions have been studied as a byproduct. The relative total free-energy differences calculated for the tautomeric pairs have been compared with those available from experimental equilibrium studies. In a number of cases, molecular dynamics (MD) simulations have been carried out in different solvents as well.

Chart 1. Numbering for the Isonicotinic Acid Pair, 4-OH-Pyridine/4-Pyridone, and Acetylacetone

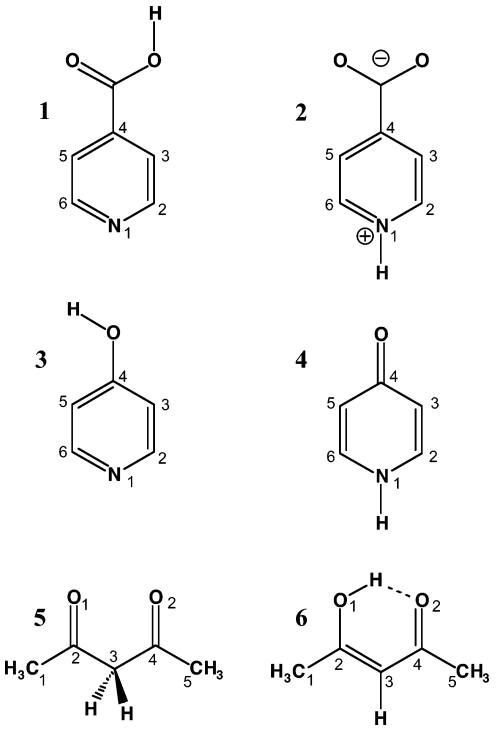

II. Methods and Calculations

Investigated structures are shown in Chart 1. Geometries of the neutral (**1**) and zwitterionic (**2**) tautomers for isonicotinic acid, 4-hydroxypyridine (**3**), 4-pyridone (**4**), and the diketo (**5**) and keto−enol (**6**) forms of acetylacetone were optimized in the gas phase as well as in tetrahydrofuran (THF), water, and methanol solvents at the DFT/B3LYP[5] (the Becke gradient-corrected three-parameter hybrid exchange and Lee−Yang−Parr correlation functionals) and integral equation formalism for the polarizable continuum model (IEF-PCM)[6]/B3LYP levels, respectively, using the 6-31G* and the 6-311++G** basis sets.[7] Calculations were performed with the aid of the Gaussian 03 software[8] and applying default dielectric constants with the IEF-PCM.

Two sets of atomic radii (reported in Table 1) were applied in forming cavities in the solvents. When the united−atom standard set, UA0 (with a scaling factor of 1.0) was used,

Table 1. Atomic Cavity Radii

	UA0 (α = 1.0)	Bondi (α = 1.2)	
	R	*R*	*R* × α
CH	2.125	1.90	2.280
CH_2	2.325	2.00	2.400
CH_3	2.525	2.00	2.400
C	1.925	1.70	2.040
=O	1.750	1.52	1.824
−OH	1.850		
N	1.830	1.55	1.860
NH	1.930		
O^-	1.750	1.52	1.824
−O		1.52	1.824
H		1.20	1.440

the CH, CH_2, and CH_3 as well as the OH and NH groups acted as single-sphere centers. The final cavity was formed by the union of the overlapping spheres around the atomic centers in the molecules. When Bondi radii[9] were used, a united-atom model was still maintained for the CH_n groups; for polar hydrogen atoms (i.e., those linked to O and N), separate centers in the cavity formation were considered, and a scaling factor of 1.2 was employed throughout.

Geometries corresponding to local energy minima were identified by all positive vibrational frequencies. Single-point energy calculations for these structures were performed at the IEF-PCM/B3LYP/6-311++G** level as well as at the IEF-PCM/QCISD(T)[10] (quadratic configuration interaction with single and double excitations and perturbative triple excitations) and CCSD(T)[11] (coupled-cluster with excitations as above) levels with the 6-31G*, 6-311++G**, and cc-pVTZ sets.[12] Relative internal energies with corrections up to the QCISD(T) level were obtained as

$$\Delta E_{\text{int}}(\text{corr}) = \Delta\langle\psi|H|\psi\rangle + \{\Delta E[\text{IEF-PCM/QCISD(T)}] - \Delta\langle\psi|H + 1/2V|\psi\rangle\} \quad (1)$$

where H and V are the Hamiltonian and the reaction field operators, respectively, and ψ is the converged wavefunction in solution (where the solvent is treated at the HF/SCF level). ΔE[IEF-PCM/QCISD(T)] includes the relative electrostatic solute−solvent interaction energy of $\Delta E_{\text{elst}} = \langle\psi|1/2V|\psi\rangle$ as well; thus, the ΔE[IEF-PCM/QCISD(T)] − $\Delta\langle\psi|H + 1/2V|\psi\rangle$ term accounts for the high-level internal energy correction. CCSD(T) corrections were obtained by using eq 1 and applying the corresponding IEF-PCM/CCSD(T) values.

Thermal corrections at the IEF-PCM/B3LYP/6-31G* level for obtaining relative internal free energies for the species were calculated in the rigid rotator, harmonic oscillator approximation[13] as

$$\Delta G_{\text{therm}}(T) = \Delta\text{ZPE} + \Delta[H_{\text{vibr}}(T) - \text{ZPE}] - T\Delta S(T) \quad (2)$$

where ZPE, $H_{\text{vibr}}(T)$, and $S(T)$ stand for the zero-point energy, the vibrational enthalpy, and the total entropy, respectively, at $T = 298$ K and $p = 1$ atm. The total relative free energy of the tautomers was calculated at the PCM level as

$$\Delta G_{\text{tot}} = \Delta E_{\text{int}} + \Delta E_{\text{elst}} + \Delta G_{\text{drc}} + \Delta G_{\text{therm}}(T) \quad (3)$$

Table 2. 12−6−1 Potential Parameters for the Pure Liquid THF in the Twist Conformation

	σ^a (Å)	ϵ^b (kcal)	*q* (atomic unit)	density (g/cm³)	heat of vaporization (kcal/mol)
O	2.900	0.140	−0.4194		
C_α	3.450	0.070	0.0879		
C_β	3.450	0.070	−0.0212		
$H_{\alpha eq}$	2.450	0.036	0.0400		
$H_{\beta ax}$	2.450	0.036	0.0464		
$H_{\beta eq}$	2.450	0.036	0.0482		
$H_{\beta ax}$	2.450	0.036	0.0084		
calcd				0.886	7.70
exp[c]				0.889	7.65

[a] The σ parameter corresponds to the atom separation when the 12−6 Lennard-Jones (LJ) potential has the zero value. [b] ϵ provides the negative of the minimum energy of the 12−6 LJ potential. [c] From ref 20.

where ΔG_{drc} is the relative nonelectrostatic free-energy term accounting for solute−solvent dispersion and repulsion energies, and for the cavity formation.

Relative solvation free energies were obtained by using the free-energy perturbation method (FEP)[14] as implemented in Monte Carlo simulations.[15] Calculations were carried out by the use of the BOSS 4.7 software.[16]

MC simulations were performed in NpT (isobaric−isothermal) ensembles at $T = 298$ K and $p = 1$ atm.[17] Water boxes including 503−505 TIP4P water molecules[18] and a single solute were considered for the aqueous solution model. The solution models with THF and methanol solvents were comprised of 262−264 solvent molecules, using three- and five-point models for methanol[19a] and THF,[19b] respectively, and a single solute. For THF, an all-atom model was also developed. Three different conformations for a THF solute were optimized at the IEF-PCM/B3LYP/6-31G* level in a THF environment, and a C_2 twisted structure was found of lowest energy. By determining the atomic charges upon the RESP fit (see below) and slightly modifying the OPLS 12−6 steric parameters, the calculated density for the solvent box comprised of 267 all-atom THF molecules as well as the heat of vaporization were in good agreement with the experimental values (Table 2). The heat of vaporization (HV) was calculated as

$$\text{HV} = (E_{\text{gas}}^{\text{int}} + RT) - [E_{\text{liq}}^{\text{int}} + E(\text{MC})/267 + pV_{\text{liq}}] \quad (4)$$

where $E_{\text{gas}}^{\text{int}} - E_{\text{liq}}^{\text{int}}$ is the change of the molar internal energy as calculated in the gas phase and in a THF environment (using the IEF-PCM) at the QCISD(T)/cc-pVTZ//B3LYP/6-31G* level. E(MC) is the MC energy for the liquid model comprised of 267 THF molecules, and V_{liq} is the THF molar volume.

Nonphysical reaction paths were selected in the FEP calculations when the tautomeric species **1**−**2**, **4**−**3**, and **5**−**6** were transformed. A nonphysical path means a gradual and contemporaneous annihilation and development of the proton involved in the tautomeric transformation at the proper sites. The reaction-coordinate parameter, λ, has values of 0 and 1 referring to the chemically correct starting and final structures

of the tautomers. When double-wide sampling[15] was used in FEP calculations, $\Delta\lambda$ was selected in the 0.0125−0.05 range in order to keep the free-energy increments at about 1 kcal/mol or less. Geometric and interaction potential parameters along the transformation path were calculated by linear interpolation between the corresponding starting and end values with a λ coupling parameter.[15] The optimized geometries for the tautomers were obtained from IEF-PCM/B3LYP/6-31G* calculations.

Interaction energies of the solution elements were calculated by using the 12−6−1-type OPLS-AA pair potential.[21] For the 12−6 steric OPLS parameters, the all-atom literature values were accepted.[21] The solvent−solvent cutoff (RCUT) and the solute−solvent cutoff (SCUT) were set to 9.75−12.0 Å and 12.0 Å, respectively. Random translation and rotation for the solute were limited to 0.1 Å and 10°, respectively. Solute trial moves were attempted every 50 steps, while volume alteration (with a maximum of 250 Å^3) was attempted every 1000 steps. Periodic boundary conditions and preferential sampling were applied with $c = 120$ in the sampling factor, $1/(R^2 + c)$, where R is the distance between the solute's reference atom and the central atom of the selected solvent molecule. With these simulation parameters, 40−60% of the newly generated configurations were accepted out of 3500 K and 5000 K configurations considered in the equilibrium and averaging phases, respectively.

The charge parameters were determined in the present study. A total of 36 ($3 \times 2 \times 2 \times 3$) charge sets were derived for each form of the three tautomeric pairs, considering three solvents (water, methanol, and THF), two cavity models (UA0 and Bondi), two fitting procedures (CHELPG[22] and RESP[23]) of the atomic charges to the in-solution molecular electrostatic potential (ELPO), and three in-solution wave functions for calculating the ELPO. Further charge sets were derived for structures **1** and **2** in vacuo for comparison. The wavefunctions were obtained either for the species optimized in the given solvent at the IEF-PCM/B3LYP/6-31G* and the IEF-PCM/B3LYP/6-311++G** levels or from IEF-PCM/B3LYP/6-311++G**//IEF-PCM/B3LYP/6-31G* single-point calculations (optimized geometries in vacuo and in solution are reported in Tables S1−S3 of the Supporting Information).

Long-range electrostatic effects (LRE) were obtained at the IEF-PCM/B3LYP level using the corresponding basis set in cases when the FEP calculations were performed with RCUT = 9.75 Å. Upon the ICUT = 2 option in the BOSS program, every solvent molecule is seen by the solute if the central atom of the solvent is within a sphere of R = SCUT around any solute atoms. Accordingly, the IEF-PCM energy providing the solute−solvent interaction energy out of the SCUT-defined volume was calculated for the tautomers with a cavity formed by interlocking spheres around the solute atoms with R = SCUT = 12 Å. In several simulations, both RCUT and SCUT were set to 12.0 Å, and the LRE was considered throughout the Ewald summation[24a] or by applying a reaction field (RF).[25] For the RF calculations, dielectric constants of 7.43, 32.63, and 78.39, relevant at $T = 298$ K, were applied in THF, methanol, and water, respectively.

The total relative free energy was calculated as

$$\Delta G_{tot} = \Delta E_{int} + \Delta G(solv) + \Delta G_{therm} \quad (5)$$

where ΔE_{int} and ΔG_{therm} are from IEF-PCM calculations and ΔG(solv) is the relative solvation free energy for the tautomers, as calculated by the FEP/MC method.

Constant pressure (p = 1 atm) and temperature ($T = 298$ K) MD simulations for 2 ns have been carried out on dimers of isonicotinic acid and its zwitterion in THF using AMBER9.[26] The THF box from the pure liquid MC simulation (see above) has been used to solvate both dimers applying periodic boundary conditions, a 12 Å cutoff, and the particle-mesh Ewald method[24b−e] to treat LRE. Both for the THF solvent and each individual solute molecule, RESP charges obtained for the IEF-PCM/B3LYP/6-31G* optimized geometries in THF using Bondi radii have been employed. A preliminary minimization (80−90 K steps) has been carried out, followed by six constant volume MD runs (using SHAKE[24f] for bonds involving H, 2 fs time-step) of 20 ps each, raising the temperature in 50 K increments until a temperature of 298 K has been reached. Then, a constant pressure equilibration (1 atm, for further 200 ps) has been carried out to approach the experimental density of 0.889 g/cm^3 for the pure THF. MD simulations in water (TIP4P) have been carried out following analogous equilibration and production phases.

III. Results and Discussion

A. Continuum Solvent Calculations. The equilibrium composition is a sensitive function of the chemical environment for many tautomeric systems. The relative standard free energy of the involved species, related to the K equilibrium constant as $-RT \ln K = \Delta G°$, changes not only through the solvation from the gas phase, but it generally varies in different solvents too.[27,28] Although continuum methods are capable of accounting for the energetic aspects of the tautomeric processes, they are inherently unable to predict the solvent structure around the solute. Both goals, thermodynamic and solution-structure characterizations of the tautomeric system, can be achieved, however, by a combined application of the ab initio/DFT continuum method and MC simulations considering explicit solvent molecules. The final relative free energies can be calculated from eq 5.

In the present MC simulations, the atom−atom interactions are calculated by pair potentials with predefined parameters. The atomic charges are the least transferable parameters, which change with the composition of the molecule including the specific atom and are affected by the chemical environment.

Coupling continuum and MC calculations, it is straightforward to resort to solvent-dependent charges. When the gas-phase HF/6-31G* charges are used, the calculated gas-phase dipole moment should be systematically overestimated, but it is likely that this value would not correctly account for the polarization both in low dielectric constant solvents and water at a time. Since the optimized geometry also changes going from the gas-phase into different solvents (torsional angles may be especially sensitive to the environment), the electron distribution also would follow these

changes. Thus, the gas-phase charges would not apply for all different solvents in principle. Neither is the use of IEF-PCM with a specific ϵ particularly appealing: this method could be advisable for obtaining charges to be used in simulations inside proteins or nucleic acids,[29] but not for dilute solutions with a wide variety of solvents. There are several other distinct methods in the literature that basically determine the atomic charges for the atom in a specific functional group or chemical environment. It is, however, outside the aim of this study to review them. Nonetheless, it is worth mentioning at least the CMx methods,[30] because their semiempirical rapid procedures are incorporated directly in BOSS[31] and have been subjected to extensive validations in solution, including the tautomeric equilibrium for 2-hydroxypyridine and 2-pyridone,[32] and for computations of absolute free energy of hydration with the TIP4P water model.[33] In our investigations, however, besides the reason put forward below, we prefer to make use of ab initio or DFT-derived ELPO charges because those fittings (only a very small fraction of the total computational time) originated from our earlier (either atom-centered or not) partial charge models in vacuo.[3a−b,34]

By the application of the PCM method, however, chemical system and solvent-dependent solute charges can be derived. In mutual modifications of the solute structure and the polarization state of the dielectric medium in PCM studies, a solute structure corresponding to a local energy minimum can be obtained if the electrostatic solute−solvent interaction is considered throughout the optimization. Because of the different solute−solvent interactions in various solvents, the optimized solute structure, and consequently the relative internal energy for the elements of a tautomeric pair, also show solvent dependence in general.[27d]

The derivation process for the atomic charges is far from being unique: even employing a single method, obtained atom-centered charges may significantly differ. In many cases, moreover, possible intramolecular hydrogen bond(s) or changes in the molecular conformation also have a non-negligible effect on the atomic charges. In addition, as mentioned above, these charges change more or less in different solvents.

If the relative internal energy has been calculated on the basis of molecular structures as obtained from a continuum approximation, a procedure for calculating the solute−solvent interaction energy/free energy in MC is consistent when the charge distribution of the solute is represented as in the continuum solvent method. These net atomic values have to mimic the overall charge distribution of the solute molecule in the given solvent. For calculating tautomeric equilibria by the FEP method, consideration of only two involved tautomeric forms suffices in general, but for determination of a rotational potential, charge derivations for a large number of conformers are needed.[35] Our goal in the present paper is to study three tautomeric systems, taking into account the effects of the applied internal parameters of the IEF-PCM method, of the basis set, and of the charge fitting procedure used to derive the in-solution relevant atomic charges on the calculated relative free energies. Results will be compared with available experimental values.

The effect of the chemical environment on the optimized structure may be assessed comparing geometric parameters from gas-phase and in-solution optimizations (Tables S1−S3, Supporting Information). Changes in the bond lengths and angles are generally monotonic in the gas phase, THF, methanol, and water-solvent series. Bond lengths may differ by up to 0.02 Å in the gas phase and in solution. For example, we found a remarkable solvent effect for the C−O distance in **1** and N−H and C_4-C_{carb} variation for **2** at the IEF-PCM/B3LYP/6-31G* level when the UA0 cavity was formed (Table S1, Supporting Information). The solvent effect is 4−5° for the OCO angle in **2** with any cavity method and with both basis sets.

The C_4-O bond of 4-pyridone changes generally by up to 0.02 Å upon solvation (Table S2, Supporting Information), but the difference is even larger in water and with the 6-311++G** basis set. Table S3 (Supporting Information) indicates a very large solvent effect on the $C_2C_3C_4O_2$ torsion angle in the diketo form with any basis set and cavity model. The solvent effect on the $O_1C_2C_3C_4$ torsion angle is 10−17° with the two basis sets.

Tables 3−5 compare the relative energies/free energies for the tautomeric pairs in the gas phase and in solution at different levels of the theory. The cavity models applied in the IEF-PCM calculations are indicated. The dominating relative energy term for the isonicotinic acid tautomers is the relative internal energy (Table 3). $\Delta G_{tot} = \Delta E_{int} + \Delta E_{elst} + \Delta G_{drc}$ is always positive and would become slightly more positive if the ΔG_{therm} were added. The positive ΔG_{tot} means that the neutral form was predicted by the IEF-PCM method as the prevailing form in solution. The prevalence of this form, however, is solvent-dependent. ΔG_{tot} decreases from THF to methanol and further decreases in water. Thus, the IEF-PCM method correctly reproduces the trend of the stability of the tautomers, indicating the increasing population of the zwitterionic form in the more polar solvent. The basis set effect on the calculated values is also important. For example, ΔG_{tot} is 5.55, 0.56, and 0.55 kcal/mol in water when the UA0 cavity is used. The decrease of 5.55 to 0.56 indicates a pure basis set effect because the two values were calculated at identical, IEF-PCM/B3LYP/6-31G*-optimized geometries with 6-31G* and 6-311++G** basis sets, respectively. The geometry effect is small, as revealed by the change of ΔG_{tot} from 0.56 to 0.55 kcal/mol, using the 6-311++G** basis sets in both cases, but on the 6-31G*- and 6-311++G**-optimized geometries.

The cavity model also affects the calculated energy terms. Using the Bondi instead of the UA0 cavity, the absolute values of both the ΔE_{int} and ΔE_{elst} terms decrease by, however, different amounts. Furthermore, the ΔG_{drc} term, although small in absolute value, is of different sign with the two cavity models. Overall, the Bondi ΔG_{tot} values obtained at a given level are about 2 kcal/mol more positive for the zwitterionic isonicotinic acid than the corresponding value calculated with the UA0 cavity. The largest problem with the IEF-PCM results for this tautomeric pair is that the method does not reproduce the switch of the tautomeric preference in water compared to THF and methanol. Experiments found[28a] about 1% and 2−4% zwitterionic isonicotinic

Table 3. Energy and Free-Energy Terms (kcal/mol) for the Zwitterionic Isonicotinic Acid Relative to the Neutral Form in the Gas Phase and from IEF-PCM/B3LYP Calculations with Different Basis Sets

B3LYP		THF		methanol		water	
6-31G*	gas phase	UA0	Bondi	UA0	Bondi	UA0	Bondi
ΔE_{int}	32.45	39.36	38.05	42.30	40.38	42.96	41.03
ΔE_{elst}		−28.60	−25.78	−35.75	−31.99	−37.29	−33.59
ΔG_{drc}		−0.11	0.08	−0.09	0.08	−0.12	0.09
ΔG_{tot}[a]		10.65	12.35	6.46	8.47	5.55	7.53
ΔG_{therm}		0.39	0.38	0.69	0.45	0.47	0.46
6-311++G**//6-31G*		UA0	Bondi	UA0	Bondi	UA0	Bondi
ΔE_{int}		37.03	35.82	40.27	38.46	40.99	39.18
ΔE_{elst}		−30.84	−28.20	−38.65	−35.11	−40.31	−36.86
ΔG_{tot}[b]		6.08	7.70	1.53	3.43	0.56	2.41
6-311++G**		UA0	Bondi	UA0	Bondi	UA0	Bondi
ΔE_{int}	29.37	37.58	36.21	40.96	38.97	41.74	39.68
ΔE_{elst}		−31.39	−28.57	−39.36	−35.62	−41.08	−37.37
ΔG_{drc}		−0.10	0.08	−0.08	0.08	−0.11	0.10
ΔG_{tot}		6.09	7.72	1.52	3.43	0.55	2.41
ΔG_{exp}[c]		2.7		2.3		−2.6	

[a] $\Delta G_{tot} = \Delta E_{int} + \Delta E_{elst} + \Delta G_{drc}$. [b] ΔG_{drc} from the 6-31G* calculations. [c] Derived from experimental compositions determined in ref 28a. The estimated uncertainty in ΔG_{exp} is up to a few tenths of a kilocalorie per mole.

Table 4. Energy and Free-Energy Terms (kcal/mol) for 4-Pyridone Relative to 4-OH-Pyridine in the Gas Phase and from IEF-PCM/B3LYP Calculations with Different Basis Sets

B3LYP		THF		methanol		water	
6-31G*	gas phase	UA0	Bondi	UA0	Bondi	UA0	Bondi
ΔE_{int}	1.51	3.85	3.37	4.98	4.30	5.24	4.51
ΔE_{elst}		−6.69	−6.17	−8.62	−8.08	−9.04	−8.45
ΔG_{drc}		−0.14	0.14	−0.13	0.12	−0.18	0.15
ΔG_{tot}[a]		−2.98	−2.66	−3.77	−3.66	−3.98	−3.79
ΔG_{therm}		0.45	0.39	0.51	0.45	0.53	0.45
6-311++G**//6-31G*		UA0	Bondi	UA0	Bondi	UA0	Bondi
ΔE_{int}		3.94	3.44	5.46	4.65	5.69	4.93
ΔE_{elst}		−8.12	−7.52	−10.69	−9.94	−11.13	−10.42
ΔG_{tot}[b]		−4.32	−3.94	−5.36	−5.17	−5.62	−5.34
6-311++G**		UA0	Bondi	UA0	Bondi	UA0	Bondi
ΔE_{int}	1.12	4.38	3.71	6.03	5.09	6.43	5.39
ΔE_{elst}		−8.55	−7.78	−11.28	−10.37	−11.90	−10.89
ΔG_{drc}		−0.15	0.13	−0.13	0.11	−0.18	0.14
ΔG_{tot}		−4.32	−3.94	−5.38	−5.17	−5.65	−5.36
ΔG_{exp}[c]	> 1.36					−4.5	

[a] $\Delta G_{tot} = \Delta E_{int} + \Delta E_{elst} + \Delta G_{drc}$. [b] ΔG_{drc} from the 6-31G* calculations. [c] Ref 28b.

acid in THF and methanol, respectively, but this tautomer population is about 95% in aqueous solution. Our best theoretical estimate is $\Delta G_{tot} = 0.56$ kcal/mol compared to −2.59 kcal/mol, derived from the experiment (Table 3).

The relative internal energies for the tautomers in the gas phase compared to the solution phase show significant changes, ranging from 6 (7) to 11 (12) kcal/mol, depending on solvent permittivity, cavity radii, and the basis set (B3LYP/6-311++G** values in parentheses). The relative stability of the zwitterionic form decreases upon interaction with the solvent, because ΔE_{int} increases. The polarity of the solvent has some effect on the relative internal energies. Whereas the ΔE_{int} values are slightly closer in the gas phase and in THF, the strong interaction of the zwitterion with polar solvents (methanol and water) leads to a distortion of the geometry (Table S1, Supporting Information) in order to make the electrostatic solute−solvent interaction energy optimally negative. The basis set effect can also be remarkable in some cases, such as for the COO group arrangement in vacuo: at the B3LYP/6-311++G** level, the carboxylate is nearly perpendicular to the ring (OCCC = 67°), whereas at the B3LYP/6-31G* level, it is located in the ring plane, as occurs in solution as well, without noticeable differences between applied levels.

Energy results for the 4-pyridone/4-OH-pyridine tautomeric pair are summarized in Table 4. Acceptance of the UA0 versus Bondi cavity has a relatively small effect on the calculated energies, although the ΔG_{drc} values are of

Table 5. Energy and Free-Energy Terms (kcal/mol) for the Diketo Relative to the Keto−Enol Form of Acetylacetone in the Gas Phase and from IEF-PCM/B3LYP Calculations with Different Basis Sets

B3LYP		THF		methanol		water	
6-31G*	gas phase	UA0	Bondi	UA0	Bondi	UA0	Bondi
ΔE_{int}	3.24	4.54	4.51	5.04	5.06	5.27	5.28
ΔE_{elst}		−2.26	−2.16	−3.17	−3.14	−3.51	−3.46
ΔG_{drc}		0.24	0.50	0.26	0.48	0.33	0.64
ΔG_{tot}[a]		2.52	2.85	2.12	2.41	2.09	2.46
ΔG_{therm}		−1.42	−1.51	−1.70	−1.98	−1.69	−1.73
6-311++ G**//6-31G*		UA0	Bondi	UA0	Bondi	UA0	Bondi
ΔE_{int}		6.82	6.79	7.39	7.42	7.66	7.67
ΔE_{elst}		−2.79	−2.70	−3.95	−3.99	−4.39	−4.41
ΔG_{tot}[b]		4.27	4.59	3.69	3.92	3.60	3.90
6-311++ G**		UA0	Bondi	UA0	Bondi	UA0	Bondi
ΔE_{int}	5.35	7.21	7.23	8.18	8.12	8.39	8.46
ΔE_{elst}		−3.25	−3.24	−4.85	−4.78	−5.22	−5.32
ΔG_{drc}		0.32	0.56	0.34	0.55	0.43	0.74
ΔG_{tot}		4.28	4.55	3.67	3.90	3.60	3.88
ΔG_{exp}[c]		0.8-1.1		0.5-0.7		−0.64	

[a] $\Delta G_{tot} = \Delta E_{int} + \Delta E_{elst} + \Delta G_{drc}$. [b] ΔG_{drc} from the 6-31G* calculations. [c] Ref 28c.

different sign in the two approximations again (see Table 3). The absolute values of the ΔE_{int} and ΔE_{elst} terms are smaller with the Bondi than with the UA0 cavity by 0.5−0.7 kcal/mol, but ΔG_{tot} differs only by 0.3−0.4 kcal/mol. Experimental results are available both in the gas phase and in solution. The gas-phase experiment indicates more than 90% 4-OH-pyridine in the tautomeric mixture, whereas 4-pyridone is almost exclusively present in aqueous solution.[28b] Our calculations predict 4-OH-pyridine as the prevailing form in the gas phase, whereas the 4-pyridone tautomer is the overwhelming fraction in all considered solutions. The calculated relative free energies show remarkable basis set dependence: $\Delta G_{tot} = -2.7$ to -3.0 and -3.9 to -4.3 kcal/mol in THF with the 6-31G* and 6-311++G** basis sets, respectively. In water, the calculated corresponding ΔG_{tot} values are -3.8 to -4.0 and -5.3 to -5.7 kcal/mol. Differences in the optimized geometries obtained with the 6-31G* and 6-311++G** basis sets have, however, negligible effect on the relative energy terms also for this tautomeric pair, as revealed by the comparison of the B3LYP/6-311++G**//B3LYP/6-31G* and B3LYP/6-311++G** results (Table 4). The consideration of the relative ΔG_{therm} values would make ΔG_{tot} less negative by 0.4−0.5 kcal/mol, still maintaining, however, the negative sign as well as a strong preference for 4-pyridone in both solvents. The geometry relaxation of the gas-phase structure is modest, especially with the Bondi cavity, in any solvent.

Concerning acetylacetone, the lowest-energy structures of its tautomers in vacuo are shown in Figure 1. While the most stable keto−enol form (**6**) is satisfactorily represented in Chart 1, with heavy atoms approximately in the same plane; the lowest-energy diketo form (**5**) significantly differs from the structure sketched in the chart both in vacuo and in solution (Figure 2). The only minimum energy structures in vacuo within 10 kcal/mol of the lowest minimum are shown in Figure 3. The second minimum (Figure 3a) is 3.5 kcal/mol less favorable than **5**, while the structure (Figure 3b) of

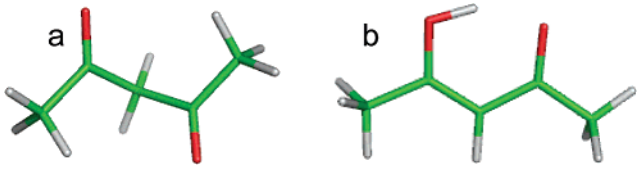

Figure 1. B3LYP/6-31G* lowest-energy structures in vacuo for the acetylacetone tautomers: (a) diketo and (b) keto−enol.

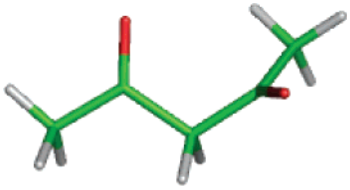

Figure 2. IEF-PCM/B3LYP/6-31G* lowest-energy structure in water for the diketo form of acetylacetone.

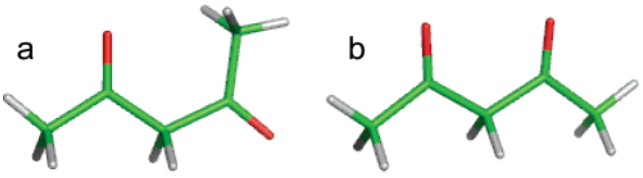

Figure 3. Additional minimum-energy structures at the B3LYP/6-31G* level for the diketo form of acetylacetone in vacuo: (a) $\Delta E = 3.48$ kcal/mol and (b) $\Delta E = 6.78$ kcal/mol.

Chart 1, a minimum indeed, is about twice as much less stable. Interestingly enough, the IEF-PCM/B3LYP/6-31G* optimization starting from either one of the aforementioned structures produces the arrangement displayed in Figure 2 which, in aqueous solution, is the most stable one, while the solvated diketo form of Figure 1a is less favorable by 0.39 kcal/mol.

IEF-PCM calculations predict that the keto−enol form of acetylacetone is more stable than the diketo tautomer both in THF and in water (Table 5). The results hardly depend

Table 6. IEF-PCM/B3LYP/6-31G* Unscaled Vibrational Frequencies (cm^{-1}) for Selected Modes of the Acetylacetone Tautomers in THF and in Water Using Different Radii

mode	THF		water	
diketo form	UA0	Bondi	UA0	Bondi
Rot C(5)H_3	136.9	136.0	112.3	114.4
Rot C(1)H_3	147.1	145.8	131.8	128.6
Stretch C(3)H (s)	3024.8	3030.0	3026.9	3033.9
Stretch C(3)H (as)	3102.2	3107.7	3086.0	3090.9
keto−enol form	UA0	Bondi	UA0	Bondi
Rot C(5)H_3	48.0	44.6	48.5	44.9
Rot C(1)H_3	117.5	117.1	116.9	116.8
Bend OH	1646.5	1655.7	1636.6	1650.5
Stretch OH	3036.8	3029.7	3046.9	3032.1
Stretch C(3)H	3197.5	3216.3	3183.9	3212.2

on the cavity calculation method, and ΔE_{int} is invariably the dominating contribution to ΔG_{tot}. The basis set effect on the calculated ΔE_{int} is more than 2 kcal/mol, but for this system, the geometric effect is also important. ΔE_{int} values, calculated with the 6-311++G** basis set with two different geometries, differ by 0.4−0.8 kcal/mol. For example, the $C_2C_3C_4O_2$ torsion angle, reported in Table S3 (Supporting Information), differs by more than 10° in the optimized geometries obtained with the two basis sets.

The positive ΔG_{tot} values predict higher free energy in the diketo as compared to the keto−enol form at any considered level. ΔG_{tot} is less positive in water than in THF, showing increasing abundance of the diketo form with increasing solvent polarity. This is in qualitative agreement with the experimental results[28c] which, however, indicate that the diketo form is the prevailing tautomer in the aqueous solution with a diketo/keto−enol ratio of 100:34. The geometry relaxation of the gas-phase structure is mainly related to the OCCC torsions in the diketo form that vary from 88/88 in vacuo to about 100/10 in solution. They, however, change insignificantly with the basis set and only moderately with the solvent polarity.

The calculated ΔG_{therm} is large for the acetylacetone tautomerism. In fact, addition of ΔG_{therm} to ΔG_{tot} reduces the latter by about 70% at the B3LYP/6-31G* level. Table 6 shows some calculated vibrational frequencies of special interest. The basic structural change in acetylacetone throughout the tautomeric transformation is that the O═C−CH_2 moiety isomerizes into the HO−C═CH substructure. The developed enolic OH group forms an intramolecular H bond with the remaining carbonyl oxygen. Thus, the C═O and C−H bonds of the diketo form disappear, and C═C and O−H bonds come into existence in the keto−enol form.

Interestingly enough, the IR spectra computed in solution (THF or water) using either the UA0 or Bondi cavities for the diketo form (Figures S1−S2 of the Supporting Information) are indistinguishable; just the maximum intensities change somewhat. The keto−enol form (Figures S3−S4, Supporting Information) shows much higher maximum intensities, especially using Bondi cavities. When the IR spectra for the keto−enol form in THF and in water are compared using the same radii (either UA0 or Bondi), there is some shift with UA0 below 1000 cm^{-1}, while the peaks within 1000 and 1500 cm^{-1} in water are slightly taller than in THF. Conversely, using Bondi radii they are still indistinguishable. The tallest peak (about 1700 cm^{-1}), present in both **5** and **6**, corresponds to the bending of the overall structures. Methyl CH stretching modes are characterized by very small peaks. Conversely, the OH stretching mode displays tall peaks. Table 6 shows that both the C−H and O−H frequencies are about 3000 cm^{-1}, producing small differences in ΔZPE. The change in ΔZPE is also relatively small due to the disappearance and appearance of a C═O and a C═C bond, respectively. The large variation in ΔG_{tot} should, in our opinion, be due to the changes in the methyl torsional vibrations. Since each tautomer bears two methyl groups, we originally guessed that their vibrational frequencies would not considerably change. The frequency analysis, however, pointed out different results. Since in the harmonic oscillator approximation low-frequency motions provide the largest vibrational entropy contribution to ΔG_{therm}, the classification of the methyl group motion as a vibration or as a hindered rotation becomes a crucial problem if the motion is remarkably different in the keto−enol compared to the diketo form. The consideration of this particular problem is out of the scope of the present study but anyway underlines how difficult a reliable comparison between calculated and experimental relative free energies (and related equilibrium constants) is in those cases when methyl groups are present in the molecule. ΔG_{therm} was smaller for the isonicotinic acid as well as for the 4-pyridone/4-OH-pyridine tautomeric pairs, where the atomic motions could be reasonably related to vibrations.

B. Atomic Charge Derivation. Despite problems regarding the sign of some ΔG_{tot} terms in the above IEF-PCM calculations, the method may still allow the derivation of atomic charges usefully applicable in MC calculations. FEP/MC calculations automatically account for the ΔG_{drc} term; thus, the crucial problem for the choice of a proper cavity-formation method is overcome in an explicit solvent study. A better estimate for the $\Delta E_{int}/\Delta E_{elst}$ balance, thus the balance of the relative internal and solvation free energy, may produce total relative free energies in acceptable agreement with the experimental values. To this aim, a number of charge sets have been derived and applied in FEP/MC calculations. The full collection of derived charges and relevant dipole moments is supplied in Tables S4−S39 of the Supporting Information. An analysis of the charges in those tables reveals the roles of the solvent, selected cavity model, basis set, and fitting method in the derivation procedure.

Charges of specific interest for the isonicotinic acid tautomers are summarized in Tables 7 and 8. A concise conclusion is that the derived in-solution values are sensitive to the basis set applied in the IEF-PCM/B3LYP calculations and the procedure, CHELPG or RESP, used for fitting atomic charges to the generated ELPO. Setting these two conditions, the charges differ only slightly, generally up to 0.03 charge units depending on the solvent, the cavity model taken in the PCM calculations, and whether the geometry was optimized with the 6-31G* or 6-311++G** basis set. The

Table 7. Isonicotinic Acid Atomic Charges Fitted to the B3LYP Electrostatic Potentials in the Gas Phase and in Solution (IEF-PCM/B3LYP/6-31G* Optimization in the Solvent Indicated, UA0 Cavity)

	gas phase				THF			
	6-31G*		6-311++G**//6-31G*		6-31G*		6-311++G**//6-31G*	
	CHELPG	RESP	CHELPG	RESP	CHELPG	RESP	CHELPG	RESP
				ZW				
N	−0.226	−0.116	−0.211	−0.087	−0.217	−0.080	−0.197	−0.046
H	0.324	0.306	0.313	0.294	0.380	0.358	0.372	0.348
C_{carb}	0.551	0.512	0.688	0.626	0.590	0.549	0.776	0.714
O	−0.595	−0.573	−0.673	−0.644	−0.685	−0.663	−0.795	−0.768
				Neutral				
N	−0.580	−0.509	−0.644	−0.594	−0.649	−0.582	−0.739	−0.700
H	0.424	0.415	0.433	0.428	0.475	0.465	0.490	0.486
C_{carb}	0.530	0.477	0.593	0.509	0.561	0.505	0.642	0.555
=O	−0.480	−0.447	−0.526	−0.486	−0.533	−0.500	−0.596	−0.556
−O	−0.550	−0.511	−0.587	−0.546	−0.569	−0.528	−0.614	−0.572
	methanol				water			
	6-31G*		6-311++G**//6-31G*		6-31G*		6-311++G**//6-31G*	
	CHELPG	RESP	CHELPG	RESP	CHELPG	RESP	CHELPG	RESP
				ZW				
N	−0.209	−0.071	−0.186	−0.038	−0.208	−0.070	−0.185	−0.036
H	0.391	0.369	0.384	0.360	0.393	0.371	0.386	0.363
C_{carb}	0.594	0.551	0.788	0.723	0.595	0.552	0.791	0.725
O	−0.700	−0.678	−0.816	−0.788	−0.703	−0.681	−0.820	−0.792
				Neutral				
N	−0.665	−0.597	−0.763	−0.724	−0.668	−0.600	−0.767	−0.729
H	0.486	0.476	0.503	0.498	0.488	0.479	0.505	0.501
C_{carb}	0.567	0.512	0.652	0.566	0.566	0.513	0.651	0.567
=O	−0.543	−0.511	−0.610	−0.571	−0.544	−0.513	−0.611	−0.574
−O	−0.572	−0.532	−0.620	−0.578	−0.572	−0.533	−0.619	−0.580

Table 8. Isonicotinic Acid Atomic Charges Fitted to IEF-PCM/B3LYP Electrostatic Potentials for the Geometries Optimized in Solution at the IEF-PCM/B3LYP/6-31G* Level in the Solvent Indicated, Bondi Cavity

	water				methanol				THF			
	6−31G*		6−311++G**		6−31G*		6−311++G**		6−31G*		6−311++G**	
	CHELPG	RESP	CHELPG	RESP	CHELPG	RESP	CHELPG	RESP	CHELPG	RESP	CHELPG	RESP
						ZW						
N	−0.194	−0.080	−0.164	−0.046	−0.205	−0.066	−0.179	−0.030	−0.211	−0.075	−0.188	−0.040
H	0.369	0.357	0.359	0.349	0.367	0.344	0.357	0.333	0.361	0.338	0.351	0.327
C_{carb}	0.595	0.590	0.786	0.759	0.586	0.545	0.774	0.710	0.579	0.541	0.759	0.700
O	−0.693	−0.683	−0.809	−0.793	−0.688	−0.667	−0.802	−0.774	−0.674	−0.653	−0.781	−0.755
						Neutral						
N	−0.655	−0.588	−0.750	−0.712	−0.652	−0.585	−0.747	−0.708	−0.639	−0.571	−0.727	−0.686
H	0.458	0.449	0.470	0.465	0.457	0.448	0.469	0.464	0.452	0.442	0.463	0.458
C_{carb}	0.562	0.508	0.641	0.555	0.560	0.507	0.639	0.553	0.555	0.501	0.631	0.546
=O	−0.529	−0.496	−0.592	−0.552	−0.527	−0.495	−0.590	−0.550	−0.519	−0.487	−0.579	−0.539
−O	−0.561	−0.521	−0.601	−0.559	−0.560	−0.521	−0.601	−0.558	−0.559	−0.519	−0.600	−0.557

gas-phase charges differ from the in-solution values remarkably. The effect of the different charge sets may be assessed from the difference in the calculated ΔG(solv) values. ΔG(solv) differs by 1 kcal/mol if the 6-31G* and the 6-311++G** Bondi/RESP sets (Table 9) are applied for the isonicotinic acid tautomers in THF. The difference in ΔG(solv) is, however, 7 kcal/mol in water despite the small deviation in the calculated dipole moments: 2.51 versus 2.60 D (neutral) and 18.53 versus 19.81 D (zwitterion) at the IEF-PCM/B3LYP/6-31G*//IEF-PCM/B3LYP/6-31G* and IEF-PCM/B3LYP/6-311++G**//IEF-PCM/B3LYP/6-31G* levels, respectively. (No experimental data are available.) Thus, whereas the global physical parameter, the dipole moment, shows a small variation with the basis set, the derived atomic charges lead to largely different relative solvation free energies. Dipole moments and ΔG(solv) values were calcu-

Table 9. Relative Solvation Free Energies, ΔG(solv)[a]

isonicotinic acid	UA0		Bondi	
ZW (**2**) − Neu (**1**)	CHELPG	RESP	CHELPG	RESP
		THF		
6-31G*[b]	−19.73 ± 0.12	−19.78 ± 0.11	−19.48 ± 0.11	−19.46 ± 0.11
RCUT = 12.0 + RF[c]				−18.06 ± 0.12
custom THF[d] + RF				−19.39 ± 0.12
Ewald[e]				−3.90 ± 0.12
6-311++G**[f]				−20.56 ± 0.12
		MeOH		
6-31G*			−38.78 ± 0.15	−38.82 ± 0.15
RCUT = 12.0 + RF			−34.97 ± 0.15	−35.75 ± 0.14
6-311++G**				−45.86 ± 0.15
		Water		
6-31G*	−51.41 ± 0.14	−52.49 ± 0.15	−47.85 ± 0.13	−50.64 ± 0.14
RCUT = 12.0 + RF				−43.89 ± 0.15
Ewald				−26.37 ± 0.16
6-311++G**	−58.08 ± 0.15	−59.60 ± 0.15	−54.89 ± 0.13	−57.45 ± 0.16
4-pyridone	UA0		Bondi	
4-py (**4**) − 4-OH (**3**)	CHELPG	RESP	CHELPG	RESP
		THF		
6-31G*	−4.35 ± 0.09	−4.26 ± 0.10	−3.92 ± 0.09	−4.21 ± 0.08
		Water		
6-31G*	−10.40 ± 0.15	−11.87 ± 0.13	−10.76 ± 0.14	−10.96 ± 0.13
6-311++G**	−14.24 ± 0.16	−14.77 ± 0.14	−13.53 ± 0.14	−13.80 ± 0.14
acetylacetone	UA0		Bondi	
diketo (**6**) − enol (**5**)	CHELPG	RESP	CHELPG	RESP
		THF		
6-31G*	−2.32 ± 0.07	−2.35 ± 0.06	−2.24 ± 0.06	−2.33 ± 0.06
6-311++G**				−2.92 ± 0.06
		Water		
6-31G*	−3.79 ± 0.19	−3.18 ± 0.15	−1.81 ± 0.18	−2.79 ± 0.15
RCUT = 12.0 + RF				−4.77 ± 0.11
6-311++G**			−3.19 ± 0.20	−2.52 ± 0.19

[a] Energies in kcal/mol. SCUT (solute−solvent cutoff) = 12.0 Å in all simulations. [b] IEF-PCM/B3LYP/6-31G* charges. RCUT (solvent−solvent cutoff) = 9.75 Å. [c] RF: reaction field applied with dielectric constant for the pure solvent. [d] All-atom custom THF solvent, see the text. [e] Ewald summation, RCUT = 12.0 Å. [f] IEF-PCM/B3LYP/6-311++G**//IEF-PCM/B3LYP/6-31G* charges, RCUT = 9.75 Å.

lated in methanol very similarly to those in water (compare Tables S8 and S9 to S4 and S5, Supporting Information; Table 9). Since the relative internal energy at the QCISD-(T) level changes by up to 0.3 kcal/mol with the two basis sets (Table 10), the total relative free energy (eq 5) strongly depends on the applied charge set in highly polar solvents.

The last important factor to be considered is the fitting procedure. Polar atomic charges calculated with the CHELPG or the RESP procedure differ in every molecule. Differences of at least 0.05 units can be found both with the 6-31G* and the 6-311++G** basis set. An a priori decision between the two methods is difficult, since both procedures provide derived atomic charges reproducing the IEF-PCM/B3LYP/6-31G* dipole moments as close as 0.01−0.02 D. Thus, FEP/MC calculations both with the CHELPG and RESP charge sets were performed for the tautomeric pairs, using different simulation parameters, as reported in Table 9.

C. Monte Carlo and Molecular Dynamics Simulations. Relative solvation free energies calculated with different charge sets are compared in Table 9. In the case of the Bondi/RESP charges, several different simulation models were considered (see also the footnote for Table 9). In the simplest model, the system corresponds to an infinitely dilute solution where the solute−solute interaction has been disregarded. This may be a reasonable approach since experimental data refer to 0.0003−0.1 molar solutions.[28] Headers 6-31G* and 6-311++G** indicate the basis set used in calculating the IEF-PCM/B3LYP molecular electrostatic potential for charge derivation. The solvent−solvent cutoff was set to 9.75 Å in these simulations. The long-range solute−solvent electrostatic interaction was corrected in the PCM approximation by calculating the interaction energy of the solute embedded in a cavity carved in the corresponding dielectric (THF, water, and methanol). The cavity was created by overlapping spheres around the solute atoms with radii of 12 Å, equal to the solute−solvent cutoff. In the second infinitely dilute solution model, the solvent−solvent cutoff was set to 12.0 Å and a reaction field was applied (RCUT = 12.0 +

Table 10. Relative Internal Energies (kcal/mol) at the QCISD(T) and CCSD(T) Levels with Different Basis Sets[a]

isonicotinic acid	THF		methanol	water	
$E_{ZW} - E_{Neu}$	UA0	Bondi	Bondi	UA0	Bondi
		QCISD(T)			
6-31G*	44.62	43.24	45.91	48.63	46.62
6-311++G**	44.15	42.93	46.13	48.35	46.53
cc-pVTZ		43.74			46.91
		CCSD(T)			
6-31G*	44.75	43.39		48.74	46.75

4-pyridone	THF		water	
$E_{4-pyr} - E_{4-OH}$	UA0	Bondi	UA0	Bondi
		QCISD(T)		
6-31G*	7.59	6.77	9.84	8.63
6-311++G**	8.91	8.17	11.43	10.32
cc-pVTZ		7.96		9.96
		CCSD(T)		
6-31G*	7.81	7.01	10.05	8.87
cc-pVTZ		8.19		10.20

acetylacetone	THF		water	
$E_{diketo} - E_{enol}$	UA0	Bondi	UA0	Bondi
		QCISD(T)		
6-31G*	0.28	0.11	1.29	1.10
6-311++G**	3.18	3.02	4.38	4.34
cc-pVTZ		5.97		7.10
		CCSD(T)		
6-31G*	0.29	0.13	1.30	1.10

[a] Geometries from IEF-PCM/B3LYP/6-31G* optimizations.

RF calculations), whereas the atomic charges were derived by means of the IEF-PCM/B3LYP/6-31G* wavefunction.

ΔG(solv) estimates with the most simulation conditions/charge parametrizations have been carried out for the isonicotinic system. The values in a row indicate the same simulation conditions with charge sets of different origin. Values in any row (also for the 4-pyridone/4-OH-pyridine and the acetylacetone system, in the lower part of Table 9) do not differ much in most cases. Thus, ΔG(solv) does not significantly depend on the origin of the charge set. The simulation conditions (RCUT = 9.75 Å, RCUT = 12.0 Å + reaction field, and Ewald summation) have, however, a remarkable effect on ΔG(solv) in most cases. The basis set, used in deriving the partial charges, also has a considerable effect on ΔG(solv).

Special attention is to be paid to the calculated ΔG(solv) values for the isonicotinic acid equilibria. Despite the large relative solvation free energies (in absolute value), the calculation is robust in aqueous solution: the forward and backward ΔG(solv) values at the 6-31G*/CHELPG/Bondi level are -47.85 ± 0.13 and 48.33 ± 0.14 kcal/mol, respectively. When the 6-311++G** charges are used, ΔG(solv) becomes more negative by 1−7 kcal/mol in the THF, methanol, and water series. In contrast, ΔG(solv) was calculated less negative with the RCUT = 12.0 + RF simulation using the 6-31G* charges. The differences are 1.4, 3.1−3.8, and 6.7 kcal/mol in the three solvents, respectively.

For the calculation of the long-range electrostatic interactions, the Ewald summation is the most widely used method nowadays. By applying this method, ΔG(solv) for the isonicotinic system was calculated to be much less negative than by means of other methods. It is implicit in the Ewald summation that the reference solution box is surrounded by an infinite number of its replica. In our systems, the equilibrium box edge was 24−33 Å, producing a nearly 0.1 molar solution concentration. Thus, the Ewald summation refers to an about 0.1 molar solution, which is much denser than the experimental one (about 0.0003 molar).[28a] The unrealistically low ΔG(solv) predicts a too positive ΔG_{tot} in eq 5 and thus predicts the preference for the neutral form in water, in contrast to the experiment. Therefore, we concluded that the Ewald summation is inapplicable for modeling the present dilute solutions and was not further considered in relation to the 4-pyridone/4-OH-pyridine system and for the keto−enol tautomerism for acetylacetone.

The ΔG(solv) values for the isonicotinic system are −18 to −21 kcal/mol in THF if Ewald summation is not applied. Then, ΔG_{tot} is at least +15 kcal/mol, taking ΔE_{int} from Tables 3 or 10 (see below). The corresponding experimental value is 2.7 kcal/mol.[28a] The large difference was attributed first to the inappropriateness of the five-point THF model,[19b] and the authors developed an all-atom THF model for the pure liquid with the density and heat of vaporization close to the experimental values (Table 2). When a solvent box comprised of 264 custom THF molecules was used, RCUT = SCUT = 12 Å was set, and a reaction field with a dielectric constant of 7.43 was applied, ΔG(solv) was calculated at −19.4 kcal/mol. This value does not differ significantly from previous values with simpler models.

The failure for predicting a ΔG(solv) value close to the experimental one initiated the idea that isonicotinic acid forms dimers in THF. Thus, 2-ns-long MD simulations have been carried out for the tautomers in the recently developed THF box. The simulations started with stacked, antiparallel solute dimers. The neutral dimer dissociated, whereas the stacked zwitterionic dimer moved into a hydrogen-bonded linear form. Thus, MD simulations indicate that the neutral form is dissolved in THF, whereas the zwitterion forms at least dimers. (Only two solute molecules were considered.) This result means that a simple transformation of a single neutral tautomer into a zwitterion throughout FEP/MC simulations is not a correct model. Although on the basis of the present MD modeling the correct ΔG(solv) has not been derived, the qualitative results indicate that the solvation in THF is more complicated than expected before. Further consideration of this problem is in progress.

An argument may be raised that the MD simulations produced an artifact for the linear zwitterionic dimer. Similar simulations have been performed for such dimers in water, and these MDs predicted largely separated neutral and zwitterionic molecules. Thus, both isonicotinic acid tautomers are present in monomeric form in water, and this feature allows the one-to-one transformation in the FEP/MC procedure. Good simulation parameters for this system provide ΔG(solv) and, ultimately, ΔG_{tot} results close to experimental

Table 11. Calculated ΔG_{tot} Values for the Zwitterionic Isonicotinic Acid Relative to the Neutral Form in Aqueous Solution[a]

		ΔG_{tot}		
Charges for ΔG(solv)		ΔE_{int} from B3LYP	ΔE_{int} from QCISD(T)	
UA0	6-31G*	6-31G*	6-31G*	
	CHELPG	−7.57	−1.90	
	RESP	−8.65	−2.98	
	6-311++G**	6-311++G**	6-311++G**	
	CHELPG	−16.21	−8.85	
	RESP	−17.73	−10.35	
Bondi	6-31G*	6-31G*	6-31G*	cc-pVTZ
	CHELPG	−5.95	−0.36	−0.07
	RESP	−8.74	−3.15	−2.86
	RCUT = 12.0 +RF	−1.99[b]	3.60[b]	3.89[b]
	6-311++G**	6-311++G**	6-311++G**	cc-pVTZ
	CHELPG	−14.84	−7.49	−7.11
	RESP	−17.40	−10.05	−9.67
exp[c]		−2.59 ± 0.05		

[a] $\Delta G_{tot} = \Delta E_{int} + \Delta G(solv) + \Delta G_{therm} + RT \ln 2$. Values in kcal/mol. Standard deviations as for the corresponding ΔG(solv) value in Table 9. [b] RESP charges. [c] From ref 28a.

results. In contrast, the ΔG_{tot} calculation fails in THF when assuming the presence of monomeric zwitterions in solution.

ΔG(solv) for the 4-pyridone/4-OH-pyridine system was calculated at the 6-31G* level both in THF and in water. Charge sets of different origin led to almost identical ΔG(solv) values of about −4 kcal/mol in THF and varied in the −10.4 to −11.9 kcal/mol range in water. When the 6-311++G** level in water was used, the calculated ΔG(solv) values scattered in the −13.5 to −14.8 kcal/mol range. The widths of the ranges in aqueous solution are very similar to each other for the two charge sets, but the 6-311++G** ΔG(solv) values are significantly more negative by about 3 kcal/mol.

For the keto−enol tautomerism of acetylacetone, the calculated ΔG(solv) in THF is nearly equal using either the 6-31G* or 6-311++G** charges. The relative solvation free energy in water varies in the −1.8 to −3.8 kcal/mol range irrespective of using the 6-31G*- or 6-311++G**-derived charges. These calculations were performed using an RCUT of 9.75 Å and PCM-based correction for the long-range electrostatic. At the RCUT = 12.0 + RF level (dielectric constant = 78.39), ΔG(solv) was calculated at −4.8 kcal/mol, which is 2 kcal/mol more negative than the corresponding 6-31G*-level value.

Thus, the use of atomic charges from fits to the in-solution B3LYP/6-31G* and B3LYP/6-311++G** ELPOs produces considerably different ΔG(solv) values in several cases, mainly in water. Still the tautomeric equilibrium constant could be predicted correctly if ΔG(solv) is combined with an appropriate ΔE_{int} term providing $\Delta G_{tot} = \Delta E_{int} + \Delta G(solv) + \Delta G_{therm}$ (plus possible corrections due to molecular symmetry) close to the experimental ΔG. Table 10 shows that not only ΔG(solv), reported in Table 9, but also ΔE_{int}(corr) can change remarkably with the applied basis set. This problem will be examined in the next section.

D. Calculation of ΔG_{tot}. ΔG_{tot} (theoretical) shows a subtle interplay of its two main components, ΔE_{int} and ΔG(solv). A recent study[27e] revealed that neither IEF-PCM/B3LYP/6-311++G**- nor IEF-PCM/MP2/6-311++G**-level calculations can account correctly for the relative internal energies in an enolimine−enaminone tautomeric equilibrium in different organic solvents. Good agreement with the experimental ΔG_{tot} was achieved, however, when ΔE_{int} was calculated as ΔE_{int}(corr). Thus, ΔE_{int}(corr) (eq 1) was calculated also in the present study with basis sets up to cc-pVTZ (Table 10).

Calculations of ΔE_{int}(corr) at the QCISD(T) and CCSD(T) levels (the IEF-PCM reference for all internal energies will be omitted henceforth) lead to small differences up to 0.2 kcal/mol in comparable cases, that is, when the same basis set was used. The results show, however, different basis set dependence of ΔE_{int}(corr) for the three studied tautomeric systems. ΔE_{int}(corr) is fairly stable in all three solvents for the isonicotinic tautomers and shows a saturation trend for the 4-pyridone/4-OH-pyridine pair but increases monotonically for the ketone−enol system with increasing the basis set. The combinations for ΔG_{tot} were taken so that the basis considered in ΔE_{int} fitted to the one used in the charge derivation for calculating ΔG(solv). Furthermore, the corresponding cavity model, UA0 or Bondi, was applied in relation to ΔE_{int} and the charge set used in determining ΔG(solv). The presented ΔG_{tot} values include the ΔG_{therm} corrections from Tables 3−5. The optimized geometry for each of the zwitterionic isonicotinic acids and 4-pyridones shows 2-fold symmetry providing a symmetry number of 2 and reducing the rotational entropy by $R \ln 2$. This effect makes ΔG_{tot} less negative by $RT \ln 2 = 0.41$ kcal/mol.

The general conclusion from the analyses of Tables 11−16 is that we have succeeded in deriving ΔG_{tot} values close to the available experimental ones, but a unique and superior combination of the ΔE_{int} and ΔG(solv) terms in calculating ΔG_{tot} has not been found. Part of the problem is the weak to strong basis set dependence of the ΔE_{int}(QCISD(T),corr) term for the studied equilibria.

Table 12. Calculated ΔG_{tot} Values for the Zwitterionic Isonicotinic Acid Relative to the Neutral Form in Methanol[a]

charges for ΔG(solv)		ΔE_{int} from B3LYP	ΔE_{int} from QCISD(T)
Bondi	6-31G*	6-31G*	6-31G*
	CHELPG	2.46	7.99
	RESP	2.42	7.95
	RCUT = 12.0 +RF	6-31G*	6-31G*
	CHELPG	5.41	11.80
	RESP	4.63	11.02
	6-311++G**	6-311++G**	6-311++G**
	RESP	−6.54	1.13
exp[b]		2.3	

[a] $\Delta G_{tot} = \Delta E_{int} + \Delta G(solv) + \Delta G_{therm} + RT \ln 2$. Values in kcal/mol. Standard deviations as for the corresponding ΔG(solv) value in Table 9. [b] ΔG_{tot} from ref 28a.

Table 13. Calculated ΔG_{tot} Values for 4-Pyridone Relative to 4-OH-Pyridine in Aqueous Solution[a]

charges in ΔG(solv)		ΔE_{int} from B3LYP	ΔE_{int} from QCISD(T)	
UA0	6-31G*	6-31G*	6-31G*	
	CHELPG	−4.22	0.38	
	RESP	−5.68	−1.09	
	6-311++G**	6-311++G**	6-311++G**	
	CHELPG	−7.61	−1.87	
	RESP	−8.14	−2.40	
Bondi	6-31G*	6-31G*	6-31G*	cc-pVTZ
	CHELPG	−5.39	−1.27	0.07
	RESP	−5.59	−1.47	−0.14
	6-311++G**	6-311++G**	6-311++G**	cc-pVTZ
	CHELPG	−7.74	−2.35	−2.71
	RESP	−8.01	−2.62	−2.98
exp[b]		−4.5		

[a] $\Delta G_{tot} = \Delta E_{int} + \Delta G(solv) + \Delta G_{therm} + RT \ln 2$. Values in kcal/mol. Standard deviations as for the corresponding ΔG(solv) value in Table 9. [b] ΔG_{tot} from ref 28b

Table 14. Calculated ΔG_{tot} Values for 4-Pyridone Relative to 4-OH-Pyridine in THF[a]

charges for ΔG(solv)		ΔE_{int} from B3LYP	ΔE_{int} from QCISD(T)	
UA0	6-31G*	6-31G*	6-31G*	
	CHELPG	0.36	4.10	
	RESP	0.45	4.19	
Bondi	6-31G*	6-31G*	6-31G*	cc-pVTZ
	CHELPG	0.25	3.65	4.84
	RESP	−0.04	3.36	4.55

[a] $\Delta G_{tot} = \Delta E_{int} + \Delta G(solv) + \Delta G_{therm} + RT \ln 2$. Values in kcal/mol. Standard deviations as for the corresponding ΔG(solv) value in Table 9.

Tables 11 and 12 summarize the calculated ΔG_{tot} values for the isonicotinic acid tautomers in water and methanol, respectively. No such table has been provided with the THF solvent where the zwitterionic tautomer forms a linear dimer according to the MD simulations. These authors ascribe the failure of FEP/MC calculations to this structural peculiarity. In contrast to the THF solutions, as stated above, the MD simulations have resulted in two, largely separated zwitterionic isonicotinic acid molecules in aqueous solution, either starting from a stacked or a linear dimer form. In aqueous solution, four ΔG_{tot} values were calculated with no more than 0.6 kcal/mol deviation from the experimental value of -2.59 ± 0.05 kcal/mol.[28a] (The best results are underscored in this and subsequent tables.) The three best results in the range of −2.86 to −3.15 kcal/mol were obtained by using the RESP/6-31G* parametrization and the ΔE_{int}(QCISD(T),corr) values. The RESP charges are clearly superior in comparison with CHELPG charges for this equilibrium. When the UA0 versus Bondi cavity is used, the calculated ΔG_{tot} changes by less than 0.2 kcal/mol, −2.98 versus −3.15 kcal/mol. When the cc-pVTZ ΔE_{int}(QCISD(T),corr) is used instead of the ΔE_{int} corrected at the QCISD(T)/6-31G* level, the improvement is 0.3 kcal/mol. The experimental ΔG_{tot} of −2.59 kcal/mol predicts a percentage zwitterionic/neutral composition of 98.8:1.2. Even with the calculated value of −3.15 kcal/mol, the corresponding ratio increases only to 99.5:0.5.

All the above values were calculated by using an RCUT = 9.75 Å and a followup LRE correction utilizing the PCM method. By applying an RCUT of 12.0 Å and a reaction field (RCUT = 12.0 + RF) throughout the calculations of the FEP increments, a value of −1.99 kcal/mol was calculated with the 6-31G*/Bondi/RESP charges. This value

Table 15. Calculated ΔG_{tot} Values for the Acetylacetone Diketone Relative to the Ketone-Enol Form in Aqueous Solution[a]

charges for ΔG(solv)		ΔE_{int} from B3LYP	ΔE_{int} from QCISD(T)	
UA0	6-31G*	6-31G*	6-31G*	
	CHELPG	−0.21	−4.19	
	RESP	0.40	−3.58	
Bondi	6-31G*	6-31G*	6-31G*	cc-pVTZ
	CHELPG	1.74	−2.44	3.56
	RESP	0.76	−3.42	2.58
	RCUT = 12.0 +RF	−1.22[b]	−5.40[b]	0.60[b]
	6-311++G**	6-311++G**	6-311++G**	cc-pVTZ
	CHELPG	2.75	−0.58	2.18
	RESP	3.42	0.09	2.85
exp[c]		−0.64		

[a] $\Delta G_{tot} = \Delta E_{int} + \Delta G(solv) + \Delta G_{therm}$. Values in kcal/mol. Standard deviations as for the corresponding ΔG(solv) value in Table 9. [b] RESP charges. [c] ΔG_{tot} from ref 28c.

Table 16. Calculated ΔG_{tot} Values for the Acetylacetone Diketone Relative to the Keto−Enol Form in THF[a]

charges for ΔG(solv)		ΔE_{int} from B3LYP	ΔE_{int} from QCISD(T)	
UA0	6-31G*	6-31G*	6-31G*	
	CHELPG	0.80	−3.46	
	RESP	0.77	−3.49	
Bondi	6-31G*	6-31G*	6-31G*	cc-pVTZ
	CHELPG	0.76	−3.64	2.22
	RESP	0.67	−3.73	2.13
	6-311++G**	6-311++G**	6-311++G**	cc-pVTZ
	RESP	2.36	−1.41	1.54
exp[b]		1.1		

[a] $\Delta G_{tot} = \Delta E_{int} + \Delta G(solv) + \Delta G_{therm}$. Values in kcal/mol. Standard deviations as for the corresponding ΔG(solv) value in Table 9. [b] ΔG_{tot} from ref 28c.

was obtained by using the B3LYP/6-31G* ΔE_{int} in Table 3. When the corresponding ΔE_{int}(QCISD(T),corr) value was applied in the $\Delta E_{int} + \Delta G$(solv) combination, a $\Delta G_{tot} = +3.60$ kcal/mol was produced without even the correct sign. Since the standard deviation for the experimental value is very small compared to the data, the value of +3.60 kcal/mol is definitely an incorrect prediction. [Standard deviations for the calculated ΔG_{tot} data in Tables 11−16 are equal to those estimated for the corresponding ΔG(solv) in Table 9.] Thus, Table 11 suggests that a fairly good estimate of ΔG_{tot} may also be obtained by a combination of ΔE_{int}-(B3LYP/6-31G*) + ΔG(solv, RCUT = 12.0 + RF). The predicted percentage composition was zwitterionic/neutral = 96.7:3.3.

Nevertheless, Table 12 contradicts this latter assumption. By applying the ΔE_{int}(B3LYP/6-31G*) + ΔG(solv, RCUT = 12.0 + RF) combination for the isonicotinic acid equilibrium in methanol, this approach overestimates the experimental ΔG_{tot} by 2−3 kcal/mol. [Although the published data in ref 28a prevent the estimation of the standard deviation for ΔG_{exp}(methanol), since the same experimental technique was applied as in the case of the aqueous solution, the standard deviation has not been expected to be larger than a few tenths of a kilocalorie per mole.] Table 12 shows that a good agreement of the calculated and experimental ΔG_{tot} was reached by the combination of ΔE_{int}(B3LYP/6-31G*) + ΔG(6-31G*/Bondi), either by applying the CHELPG or the RESP charges. By using the ΔE_{int}(QCISD(T)/6-31G*,corr) relative internal energy, the predicted ΔG_{tot} has been strongly overestimated. In contrast, however, a somewhat underestimated value of 1.13 kcal/mol (including ΔLRE as in all cases where the RF term is not explicitly indicated) was calculated with the 6-311++G**/Bondi/RESP charge parametrization and using the ΔE_{int}(QCISD(T)/6-311++G**,-corr) relative internal energy. All calculations (except one, $\Delta G_{tot} = -6.54$ kcal/mol) predict the preference of the neutral form; the best result is neutral/zwitterionic = 98.4:1.6 compared to the experimental composition of 98:2.

The 4-pyridone/4-OH-pyridine calculations in aqueous solution (Table 13) predict a stable preference for 4-pyridone. This table also indicates that much better agreement with the experimental value can be reached by utilizing the ΔE_{int}-(B3LYP/6-31G*) instead of the ΔE_{int}(QCISD(T)/6-31G*,-corr) term in calculating ΔG_{tot}. The best result (B3LYP/6-31G*) was obtained with the CHELPG charges; results with the RESP charges are too negative by about 1 kcal/mol with respect to the experiment. The experimental 4-pyridone/4-OH-pyridine composition in aqueous solution is 2000:1 compared with our best calculated ratio of 1247:1.

The solvent effect is large for the 4-pyridone/4-OH-pyridine tautomeric equilibria. The gas-phase equilibrium constant $K < 0.1$ increases to 2000 in aqueous solution.[28b]

The dipole moment measured for the system subject to tautomerization was reported as 6.0−6.3 D in dioxane.[36a,b] Our calculated dipole moments for 4-pyridone and 4-OH-pyridine are 8.8 and 3.5 D, respectively, at the IEF-PCM/B3LYP/6-31G* level with the Bondi cavity in THF. The corresponding values are 9.4 and 3.7 D in aqueous solution (compare Tables S6 and S7 with S14 and S15 in the Supporting Information). The experimental dipole moment about halfway between the calculated values for the pure tautomers suggests a nearly 1:1 equilibrium composition in the low-dielectric constant solvent ($\epsilon = 2.21$ for dioxane[20]). Thus, we may conclude that the equilibrium is shifted from a 4-OH-pyridine preference in the gas phase to a nearly equal concentration of both tautomers in dioxane and to an overwhelming preference for 4-pyridone in aqueous solution. Our computational results in the THF solvent ($\epsilon = 7.43$) fit in this series.

Table 14 indicates a total free energy of −0.04 to +0.45 kcal/mol for 4-pyridone relative to 4-OH-pyridine in THF, when the ΔE_{int}(B3LYP/6-31G*) term has been used for calculating ΔG_{tot}. These values provide 4-pyridone/4-OH-pyridine ratios from 1:0.9 to 1:2.1. A very small 4-pyridone fraction is predicted in the equilibrium mixture when the ΔG_{tot} is calculated by accepting the (QCISD(T)/6-31G*,-corr) relative internal energy. With these ΔE_{int} values, the ratio varies between 1:292 and 1:3553. These latter values are exceedingly smaller than the gas-phase experimental ratio. By recognizing that the dielectric constant for THF is much closer to that for dioxane than to that for water, the authors consider a ratio between 1:1 and 1:2 as a realistic prediction in THF.

The acetylacetone tautomerization was studied experimentally in a large number of solvents.[28c] The *K*(enol/diketone) equilibrium constant gradually decreases with increasing solvent polarity. The *K* values were determined (studying 0.01 molar solutions) as 48, 6.5, 3.3, and 0.34 in hexane, THF, methanol, and water, respectively. The derived ΔG_{exp} is −0.64 kcal/mol for the diketone form relative to the enol tautomer in aqueous solution (Table 15). The theoretical calculations for this equilibrium provide ΔG_{tot} values in the broad range of −5.40 to +3.56 kcal/mol. The large variation is a consequence of the different combinations of the ΔE_{int} scattering in a range of 6.6 kcal/mol (Tables 5 and 9) and the ΔG(solv) term varying by up to 3.0 kcal/mol in different FEP/MC calculations. The large positive values for ΔG_{tot} are most likely incorrect by assuming that at least the sign of the ΔG_{exp} is correct. Unless there was a systematic error in the experiment, the equal equilibrium constants derived at two different concentrations (0.01 and 0.1 molar) suggest the stable composition with about 3:1 diketone/enol.

Table 9 shows that the ΔG(solv) values are robust at the 6-31G*/RESP level and hardly change upon the charge set derived on the basis of calculations with UA0 or Bondi cavity. In contrast, ΔG(solv) calculated with CHELPG charges changes by 2 kcal/mol whether the charge set was obtained with the UA0 or the Bondi cavity via the IEF-PCM calculations. Except a small negative value of −0.21 kcal/mol for ΔG_{tot}, the other three values calculated by means of the ΔE_{int}(B3LYP/6-31G*) relative internal energy are all positive. When the ΔE_{int}(B3LYP/6-311++G**) relative energies are used with the Bondi cavity and the corresponding charge sets, ΔG_{tot} becomes even more positive. Consistently negative ΔG_{tot} values were calculated by applying the ΔE_{int}(QCISD(T)/6-31G*,corr) relative energies, but the derived relative free energies are too negative. The very good $\Delta G_{tot} = -0.58$ kcal/mol was obtained by a combination of the ΔE_{int}(QCISD(T)/6-311++G**,corr) and the 6-311++G**/Bondi/CHELPG ΔG(solv) terms. The results, however, might be a consequence of fortuitous error cancellations; this specific combination led to poor or moderately good results at most for other systems (Tables 11 and13).

The ΔG_{tot} value derived by means of the RCUT = 12.0 + RF/ΔG(solv) term (Table 9) in combination with the ΔE_{int}-(B3LYP/6-31G*) relative internal energy is −1.22 kcal/mol, deviating only by 0.6 kcal/mol from the experimental value. A similar deviation (although in the opposite direction) was obtained by this combination for the isonicotinic acid equilibrium in aqueous solution. Also, the correct sign for ΔG_{tot} (but a deviation of 2−3 kcal/mol) was found, however, for the latter equilibrium in methanol. Further studies are necessary for exploring how robust this combination is for different equilibrium systems.

In calculating ΔG_{tot}, only the IEF-PCM/B3LYP/6-31G* minimum energy structures were considered both for the enol and the diketone. Although the IEF-PCM calculations predicted two structures (Figures 1a and 2) for the diketone differing only by 0.39 kcal/mol, FEP/MC calculations provided an increase of 2.37 ± 0.13 kcal/mol in ΔG(solv) for the Figure 1a structure. Since this conformer population in the diketone mixture is less than 2%, it has been disregarded and will not be the subject of further consideration.

The computational results for the acetylacetone tautomeric equilibrium in THF solvent (Table 16) may be summarized so that the ΔE_{int}(B3LYP/6-31G*) + 6-31G*/ΔG(solv) combination provides good agreement with the experimental values, whereas other combinations either lead to exaggeration of the ΔG_{tot} or even provide the wrong sign for the relative free energy. Application of the ΔE_{int}(QCISD(T)/6-31G*,corr) term leads to a ΔG_{tot} of −3.46 to −3.73 kcal/mol compared to the value of 0.8−1.1 kcal/mol derived from the experimental *K* value. When ΔE_{int}(QCISD(T)/cc-pVTZ,-corr) is used, the sign is correct, but ΔG_{tot} becomes too positive: 1.54−2.22 kcal/mol.

Our calculated dipole moments at the IEF-PCM/B3LYP/6-31G* level (using either UA0 or Bondi cavity) range from 3.7 D (keto−enol) and 4.3 D (diketone) in THF to 3.9 D (keto−enol) and 5.1 D (diketone) in water (Tables S16−S21 in the Supporting Information). Thus, on the basis of these theoretical values, the more polar tautomer becomes the preferred one in the larger polarity solvent. The same trend was found for the other two aforementioned tautomeric systems as well.

An experimental study by Ghanadzadeh et al.[37] alerts, however, that dipolar molecules may form dimers in nonpolar solvents, causing an increased measurable value for the dipole moment of the solute. The type of the association depends on the functional group; ketones form dimers with

parallel C═O moments. The diketone form of acetylacetone has C═O bond moments pointing away depending on the chemical environment: the conformation is largely different in the gas phase and in solution (see above). Association may also be possible for 4-pyridone and, as it has been explored, for the zwitterionic isonicotinic acid in THF. These authors have concluded from the present study that a fast molecular dynamics exploration of the association character (monomer vs dimer) is useful prior to the application of the DFT + FEP/MC method for calculating ΔG_{tot} in nonpolar solvents.

A general comparison of the polarizable continuum dielectric and explicit solvent approaches indicates that the IEF-PCM method saves the sign of the ΔG_{tot} term in different solvents (Tables 3−5), whereas the DFT/FEP/MC procedure is more flexible (Tables 9−16). The experimental results seemingly are precise enough for considering at least the switch of the sign for ΔG to be significant. The IEF-PCM method did not predict the switch of the tautomeric preference for isonicotinic acid in water. As discussed above, the positive ΔE_{int} terms from B3LYP calculations determine the sign of ΔG_{tot} in all three solvents (Table 3), although the trend of the tautomeric preference has been correctly predicted. By considering thermal and symmetry corrections for the 4-pyridone/4-OH-pyridine system, ΔG_{tot} was predicted to be $-3.79 + 0.86 = -2.93$ kcal/mol at the IEF-PCM/B3LYP/6-31G*/Bondi theoretical level, in qualitative agreement with the experimental value of −4.5 kcal/mol in aqueous solution. The IEF-PCM/B3LYP/6-31G* ΔG_{tot} values of 1.1−1.3 kcal/mol, including thermal corrections, for the acetylacetone equilibrium are in good agreement with the experimental 0.8−1.1 kcal/mol in THF. The calculated positive sign of ΔG_{tot} disagrees, however, with the sign of the experimental value for acetylacetone in aqueous solution.

In contrast, by calculating ΔG_{tot} as $\Delta G_{tot} = \Delta E_{int}$(IEF-PCM/B3LYP/6-31G*) + 6-31G*/ΔG(solv) + ΔG_{therm} + (symmetry correction) in the framework of the DFT/FEP/MC procedure, deviations from experimental values were generally less than 1 kcal/mol. With abs(ΔG_{exp}) > 2 kcal/mol, the deviation was small and the predicted sign for ΔG was correct. In cases with abs(ΔG_{exp}) < 1 kcal/mol, the sign was not correctly determined in some cases. The total relative free energy for the isonicotinic acid equilibrium in aqueous solution was very well estimated, however, only when the QCISD(T)/cc-pVTZ relative internal energy was used.

IV. Conclusions

A systematic study has been performed for estimating the relative free energies of the tautomeric pairs in equilibria for isonicotinic acid in THF, methanol, and water, and for the 4-OH-pyridine and acetylacetone in THF and aqueous solution. Isonicotinic acid can form a zwitterionic tautomer, whereas the tautomers are common organic structures in the other two equilibria considered. After performing in-solution geometry optimizations at the IEF-PCM/B3LYP level for the three pairs of tautomers, the effects of the solvent, basis set, cavity model, and charge fitting procedure on the resulting total relative free energy were studied. Corresponding geometries obtained at the IEF-PCM/B3LYP/6-31G* and 6-311++G** levels differ moderately both in tetrahydrofuran and in water solvents, but some torsion angles may deviate considerably from their gas-phase values.

Atomic charges fitted to the in-solution ELPO show small variations in different solvents, if all other calculation conditions are kept unchanged. The UA0 cavity model, or a model with explicit consideration of the polar hydrogens and applying scaled Bondi radii, has a small effect on the derived atomic charges as well. In contrast, the fitting procedure, CHELPG or RESP, has a considerable effect on the calculated values. The CHELPG fit produces more separated atomic charges than those obtained with the RESP procedure, although both derivation methods reproduce well the overall in-solution dipole moment of the selected species. The charges increase up to 20% in absolute value when the 6-311++G** rather than the 6-31G* basis set is used in the IEF-PCM/B3LYP calculations. The relative solvation free energies from FEP/MC calculations lead to differences up to about 3 kcal/mol with RCUT = 9.75 Å in aqueous solution, using different cavity and charge derivation methods and with either 6-31G* or 6-311++G** basis sets. In contrast, ΔG(solv) terms are fairly insensitive to these simulation parameters in THF. When RCUT = 12.0 Å and a reaction field throughout the FEP/MC process are considered, the calculated ΔG(solv) deviates by 1.5−3.0 kcal/mol from the values above.

ΔG_{tot}, as calculated from $\Delta E_{int} + \Delta G$(solv) + ΔG_{therm} + (symmetry correction), strongly depends on the accepted value for ΔE_{int}. In order to predict the relative free energy for the zwitterionic isonicotinic acid tautomer in close agreement with the experimental values in aqueous solution, ΔE_{int} had to be calculated at the IEF-PCM/QCISD(T)/cc-pVTZ//IEF-PCM/B3LYP/6-31G* level. Consideration of the IEF-PCM/B3LYP/6-31G* ΔE_{int} value suffices, however, in methanol. Molecular dynamics simulations pointed out that isonicotinic acid forms a dimeric zwitterion in THF, in contrast to what happens in aqueous solution, and this structural peculiarity has been interpreted by these authors as the reason for the considerable failure of the ab initio/DFT + FEP/MC method in this particular case.

In cases of the 4-OH-pyridine and acetylacetone tautomeric systems, the calculated ΔG_{tot} values, by considering the ΔE_{int} (IEF-PCM/B3LYP/6-31G*) and 6-31G*/ΔG(solv) contributions, are close to the available experimental values both in THF and in aqueous solution. The agreement is good in cases of abs(ΔG_{exp}) > 2 kcal/mol, whereas the deviation of the calculated and experimental ΔG values may amount to about 1 kcal/mol with abs(ΔG_{exp}) < 1 kcal/mol.

Acknowledgment. The authors are grateful to David Case for granting them permission to use the AMBER9 program. P.I.N. thanks the Ohio Supercomputer Center for the granted computer time used for some of the QCISD(T) and CCSD(T) calculations.

Supporting Information Available: Geometric parameters optimized in solution at the IEF-PCM/B3LYP level with two basis sets (6-31G* and 6-311++G**) for the systems considered (Tables S1−S3); CHELPG (Tables S4−

S21) and RESP (Tables S22−S39) charges and relevant dipole moments in solution on the geometries optimized in solution at the IEF-PCM/B3LYP6-31G* or 6-311++G** level using UA0 and Bondi cavities (single-point IEF-PCM/B3LYP/6-311++G**//IEF-PCM/B3LYP/6-31G* results are also included); in the last line of the CHELPG tables (S4−S21), the dipole moments computed from the real densities in solution are reported; IR spectra in THF and aqueous solution for the acetylacetone tautomers with both cavities (Figures S1−S4). This material is available free of charge via the Internet at http://pubs.acs.org.

References

(1) Hutter, J.; Alavi, A.; Deutsch, T.; Bernasconi, M.; Goedecker, S.; Marz, D.; Tuckermann, M.; Parrinello, M. *CPMD*; MPI fur Festkorperforschung, and IBM Zurich Research Laboratory: Stutggart, Germany, 1995−1999.

(2) (a) Laio, A.; Vondele, J. V.; Röthlisberger, U. *J. Chem. Phys.* **2002**, *116*, 6941−6947. (b) Andreoni, W. In *3D QSAR in Drug Design: Ligand−Protein Interactions and Molecular Similarity*; Kubinyi, H., Folkers, G., Martin, Y. C., Eds.; Kluwer/ESCOM: Dordrecht, The Netherlands, 1998; Vol. 2, pp 161−167. (c) Andreoni, W.; Curioni, A.; Mordasini, T. *IBM J. Res. Dev.* **2001**, *45*, 397−407 and references therein.

(3) (a) Bonaccorsi, R.; Petrongolo, C.; Scrocco, E.; Tomasi, J. *Theor. Chim. Acta* **1971**, *20*, 331−342. (b) Alagona, G.; Cimiraglia, R.; Scrocco, E.; Tomasi, J. *Theor. Chim. Acta* **1972**, *25*, 103−119. (c) Kollman, P. A.; Hayes, D. M. *J. Am. Chem. Soc.* **1981**, *103*, 2955−2961. (d) Warshel, A.; Lappicirella, A. *J. Am. Chem. Soc.* **1981**, *103*, 4664−4673. (e) Alagona, G.; Desmeules, P.; Ghio, C.; Kollman, P. A. *J. Am. Chem. Soc.* **1984**, *106*, 3623−3632. (f) Singh, U. C.; Kollman, P. A. *J. Comput. Chem.* **1986**, *7*, 718−730. (g) Field, M. J.; Bash, P. A.; Karplus, M. *J. Comput. Chem.* **1990**, *11*, 700−733. (h) Ferenczy, G. G.; Rivail, J.-L.; Surján, P. R.; Náray-Szabó, G. *J. Comput. Chem.* **1992**, *13*, 830−837. (i) Gao, J.; Xia, X. *Science* **1992**, *258*, 631−635. (j) Maseras, F.; Morokuma, K. *J. Comput. Chem.* **1995**, *16*, 1170−1179. (k) Stanton, R. V.; Hartsough, D. S.; Merz, K. M., Jr. *J. Comput. Chem.* **1995**, *16*, 113−128.

(4) See, for example: (a) Nagy, P. I.; Dunn, W. J., III.; Alagona, G.; Ghio, C. *J. Am. Chem. Soc.* **1991**, *113*, 6719−6729. (b) Nagy, P. I.; Dunn, W. J., III.; Alagona, G.; Ghio, C. *J. Am. Chem. Soc.* **1992**, *114*, 4752−4758. (c) Nagy, P. I.; Dunn, W. J., III.; Alagona, G.; Ghio, C. *J. Phys. Chem.* **1993**, *97*, 4628−4642. (d) Nagy, P. I.; Alagona, G.; Ghio, C. *J. Am. Chem. Soc.* **1999**, *121*, 4804−4815. (e) Nagy, P. I.; Alagona, G.; Ghio, C.; Takács-Novák, K. *J. Am. Chem. Soc.* **2003**, *125*, 2770−2785.

(5) (a) Becke, A. D. *J Chem. Phys.* **1993**, *98*, 5648−5652. (b) Lee, C.; Yang, W.; Parr, R. G. *Phys. Rev. B: Condens. Matter Mater. Phys.* **1988**, *37*, 785−789.

(6) (a) Miertus, S.; Scrocco, E.; Tomasi, J. *Chem. Phys.* **1981**, *55*, 117−129. (b) Miertus, S.; Tomasi, J. *Chem. Phys.* **1982**, *65*, 239−245. (c) Tomasi, J.; Persico, M. *Chem. Rev.* **1994**, *94*, 2027−2094. (d) Tomasi, J.; Mennucci, B.; Cammi, R. *Chem. Rev.* **2005**, *105*, 2999−3094.

(7) Hehre, W. J.; Radom, L.; Schleyer, P. v. R.; Pople, J. A. *Ab Initio Molecular Orbital Theory*; Wiley: New York, 1986.

(8) Frisch, M. J.; Trucks, G. W.; Schlegel, H. B.; Scuseria, G. E.; Robb, M. A.; Cheeseman, J. R.; Montgomery, J. A., Jr.; Vreven, T.; Kudin, K. N.; Burant, J. C.; Millam, J. M.; Iyengar, S. S.; Tomasi, J.; Barone, V.; Mennucci, B.; Cossi, M.; Scalmani, G.; Rega, N.; Petersson, G. A.; Nakatsuji, H.; Hada, M.; Ehara, M.; Toyota, K.; Fukuda, R.; Hasegawa, J.; Ishida, M.; Nakajima, T.; Honda, Y.; Kitao, O.; Nakai, H.; Klene, M.; Li, X.; Knox, J. E.; Hratchian, H. P.; Cross, J. B.; Bakken, V.; Adamo, C.; Jaramillo, J.; Gomperts, R.; Stratmann, R. E.; Yazyev, O.; Austin, A. J.; Cammi, R.; Pomelli, C.; Ochterski, J. W.; Ayala, P. Y.; Morokuma, K.; Voth, G. A.; Salvador, P.; Dannenberg, J. J.; Zakrzewski, V. G.; Dapprich, S.; Daniels, A. D.; Strain, M. C.; Farkas, O.; Malick, D. K.; Rabuck, A. D.; Raghavachari, K.; Foresman, J. B.; Ortiz, J. V.; Cui, Q.; Baboul, A. G.; Clifford, S.; Cioslowski, J.; Stefanov, B. B.; Liu, G.; Liashenko, A.; Piskorz, P.; Komaromi, I.; Martin, R. L.; Fox, D. J.; Keith, T.; Al-Laham, M. A.; Peng, C. Y.; Nanayakkara, A.; Challacombe, M.; Gill, P. M. W.; Johnson, B.; Chen, W.; Wong, M. W.; Gonzalez, C.; Pople, J. A. *Gaussian 03*, Revision C.02; Gaussian, Inc.: Wallingford, CT, 2004.

(9) Bondi, A. *J. Phys. Chem.* **1964**, *68*, 441−451.

(10) Pople, J. A.; Head-Gordon, M.; Raghavachari, K. *J. Chem. Phys.* **1987**, *87*, 5968−5975.

(11) CCSD is described in: Purvis, G. D.; Bartlett, R. J. *J. Chem. Phys.* **1982**, *76*, 1910−1918. The extension to noniterative inclusion of triple excitations appears in: Raghavachari, K.; Trucks, G. W.; Pople, J. A.; Head-Gordon, M. *Chem. Phys. Lett.* **1989**, *157*, 479−483.

(12) Dunning, T. H., Jr. *J. Chem. Phys.* **1989**, *90*, 1007−1023.

(13) McQuarrie, D. A. *Statistical Mechanics*; University Science Book: Sausalito, CA, 2000.

(14) Zwanzig, *J. Chem. Phys*. **1954**, *22*, 1420−1426.

(15) Jorgensen, W. L.; Ravimohan, C. *J. Chem. Phys.* **1985**, *83*, 3050−3054.

(16) Jorgensen, W. L. *BOSS*, version 4.7; Yale University: New Haven, CT, 2006.

(17) (a) Jorgensen, W. L.; Madura, J. D. *J. Am. Chem. Soc.* **1983**, *105*, 1407−1413. (b) Jorgensen, W. L.; Swenson, C. J. *J. Am. Chem. Soc.* **1985**, *107*, 1489−1496. (c) Jorgensen, W. L.; Gao, J. *J. Phys. Chem.* **1986**, *90*, 2174−2182. (d) Jorgensen, W. L.; Briggs, J. M.; Contreras, M. L. *J. Phys. Chem.* **1990**, *94*, 1683−1686.

(18) (a) Jorgensen, W. L.; Chandrasekhar, J.; Madura, J. D.; Impey, R. W.; Klein, M. L. *J. Chem. Phys.* **1983**, *79*, 926−935. (b) Jorgensen, W. L.; Madura, J. D. *Mol. Phys.* **1985**, *56*, 1381−1392.

(19) (a) Jorgensen, W. L. *J. Phys. Chem.* **1986**, *90*, 1276−1284. (b) Briggs, J. M.; Matsui, T.; Jorgensen, W. L. *J. Comput. Chem.* **1990**, *11*, 958−971.

(20) Riddick, J. A.; Bunger, W. B.; Sakano, T. K. *Organic Solvents*; Wiley: New York, 1986.

(21) Jorgensen, W. L.; Maxwell, D. S.; Tirado-Rives, J. *J. Am. Chem. Soc.* **1996**, *118*, 11225−11236.

(22) Breneman, C. M.; Wiberg, K. B. *J. Comput. Chem.* **1990**, *11*, 361−373.

(23) (a) Bayly, C. I.; Cieplak, P.; Cornell, W. D.; Kollman, P. A. *J. Phys. Chem.* **1993**, *97*, 10269−10280. (b) Cornell, W. D.; Cieplak, P.; Bayly, C. I.; Kollman, P. A. *J. Am. Chem. Soc.* **1993**, *115*, 9620−9631.

(24) (a) Ewald, P. P. *Ann. Phys.* **1921**, *64*, 253−287. (b) Darden, T.; York, D.; Pedersen, L. *J. Chem. Phys.* **1993**, *98*, 10089−10092. (c) Essmann, U.; Perera, L.; Berkowitz, M. L.;

Darden, T.; Lee, H.; Pedersen, L. G. *J. Chem. Phys*. **1995**, *103*, 8577−8593. (d) Crowley, M. F.; Darden, T. A.; Cheatham, T. E., III; Deerfield, D. W., II. *J. Supercomput*. **1997**, *11*, 255−278. (e) Sagui, C.; Darden, T. A. In *Simulation and Theory of Electrostatic Interactions in Solution*; Pratt, L. R., Hummer, G., Eds.; AIP: Melville, NY, 1999; pp 104−113. (f) Ryckaert, J.-P.; Ciccotti, G.; Berendsen, H. J. C. *J. Comput. Phys*. **1977**, *23*, 327−341.

(25) Essex, J. W.; Jorgensen, W. L. *J. Phys. Chem*. **1995**, *99*, 17956−17962.

(26) Case, D. A.; Darden, T. A.; Cheatham, T. E., III; Simmerling, C. L.; Wang, J.; Duke, R. E.; Luo, R.; Merz, K. M.; Pearlman, D. A.; Crowley, M.; Walker, R. C.; Zhang, W.; Wang, B.; Hayik, S.; Roitberg, A.; Seabra, G.; Wong, K. F.; Paesani, F.; Wu, X.; Brozell, S.; Tsui, V.; Gohlke, H.; Yang, L.; Tan, C.; Mongan, J.; Hornak, V.; Cui, G.; Beroza, P.; Mathews, D. H.; Schafmeister, C.; Ross, W. S.; Kollman P. A. *AMBER 9*; University of California: San Francisco, CA, 2006.

(27) See, for example: (a) Kwiatkowski, J. S.; Zielinski, T. J.; Rein, R. *Adv. Quantum. Chem*. **1986**, *18*, 85−130. (b) Cieplak, P.; Bash, P.; Singh, U. C.; Kollman, P. A. *J. Am. Chem. Soc.* **1987**, *109*, 6283−6289 and references therein. (c) Fabian, W. M. F.; Antonov, L.; Nedeltcheva, D.; Kamounah, F. S.; Taylor, P. J. *J. Phys. Chem. A* **2004**, *108*, 7603−7612. (d) Nagy, P. I.; Tejada, F. R.; Messer, W. S., Jr. *J. Phys. Chem. B* **2005**, *109*, 22588−22602. (e) Nagy, P. I.; Fabian, W. M. F. *J. Phys. Chem. B* **2006**, *110*, 25026−25032.

(28) (a) Nagy, P. I.; Takács-Novák, K. *J. Am. Chem. Soc.* **1997**, *119*, 4999−5006. (b) Beak, P. *Acc. Chem. Res.* **1977**, *10*, 186−192 and references therein. (c) Moriyasu, M.; Kato, A.; Hashimoto, Y. *J. Chem. Soc., Perkin Trans. II* **1986**, 515−520.

(29) Duan, Y.; Wu, C.; Chowdhury, S.; Lee, M. C.; Xiong, G.; Zhang, W.; Yang, R.; Cieplak, P.; Luo, R.; Lee, T.; Caldwell, J.; Wang, J.; Kollman, P. *J. Comput. Chem*. **2003**, *24*, 1999−2012.

(30) (a) Storer, J. W.; Giesen, D. J.; Cramer, C. J.; Truhlar, D. G. *J. Comput.-Aided Mol. Des*. **1995**, *9*, 87−110. (b) Li, J.; Zhu, T.; Cramer, C. J.; Truhlar, D. G. *J. Phys. Chem. A* **1998**, *102*, 1820−1831. (c) Thompson, J. D.; Cramer, C. J.; Truhlar, D. G. *J. Comput. Chem*. **2003**, *24*, 1291−1304.

(31) (a) Jorgensen, W. L.; Tirado-Rives, J. *J. Comput. Chem.* **2005**, *26*, 1689−1700. (b) Jorgensen, W. L.; Tirado-Rives, J. *Proc. Natl. Acad. Sci. U.S.A.* **2005**, *102*, 6665−6670.

(32) Kaminski, G. A.; Jorgensen, W. L. *J. Phys. Chem. B* **1998**, *102*, 1787−1796.

(33) Udier-Blagovic, M.; Morales de Tirado, P.; Pearlman, S. A.; Jorgensen, W. L. *J. Comput. Chem.* **2004**, *25*, 1322−1332.

(34) (a) Alagona, G.; Pullman, A.; Scrocco, E.; Tomasi, J. *Int. J. Peptide Protein Res*. **1973**, *5*, 251−259. (b) Pullman, A.; Alagona, G.; Tomasi, J. *Theor. Chim. Acta* **1974**, *33*, 87−90. (c) Ghio, C.; Scrocco, E.; Tomasi, J. In *Environmental Effects on Molecular Structure and Properties*; Pullman, B., Ed.; Reidel: Dordrecht, Holland, 1975; pp 329−342.

(35) Alagona, G.; Ghio, C.; Nagy, P. I. *J. Chem. Theory Comput.* **2005**, *1*, 801−816.

(36) (a) Leis, D. G.; Curran, B. C. *J. Am. Chem. Soc.* **1945**, *67*, 79−81. (b) Albert, A.; Phillips, J. N. *J. Chem. Soc.* **1956**, 1294−1304.

(37) Ghanadzadeh Gilani, A.; Mamaghani, M.; Anbir, L. *J. Sol. Chem*. **2003**, *32*, 625−636.

CT6002252